We are IntechOpen, the world's leading publisher of Open Access books
Built by scientists, for scientists

6,900
Open access books available

185,000
International authors and editors

200M
Downloads

154
Countries delivered to

Our authors are among the

TOP 1%
most cited scientists

12.2%
Contributors from top 500 universities

CLARIVATE ANALYTICS
BOOK CITATION INDEX
INDEXED

WEB OF SCIENCE™

Selection of our books indexed in the Book Citation Index
in Web of Science™ Core Collection (BKCI)

Interested in publishing with us?
Contact book.department@intechopen.com

The Formation of Silicon Carbide in the SiC$_x$ Layers (x = 0.03–1.4) Formed by Multiple Implantation of C Ions in Si

Kair Kh. Nussupov and Nurzhan B. Beisenkhanov
Kazakh-British Technical University
Kazakhstan

1. Introduction

Promising application of thin-film technology is the synthesis of SiC, possessing such valuable properties as high hardness (33400 Mn/m^2), chemical resistance, high melting point (2830°C), wide bandgap (2.3–3.3 eV), etc (Lindner , 2003). Unfortunately, since it is still difficult to grow SiC material of crystalline quality to meet requirements for a large scale industrial application, small-size and high-cost SiC wafers severely limit their applications at present (Liangdeng et al., 2008). Doped with different impurities, silicon carbide is used in semiconductor technology (Yan et al., 2000; Chen et al., 2003). Field-effect transistors, diodes and other electronic devices based on SiC have several advantages compared to similar silicon devices. Among them, the opportunity to work at temperatures up to 600°C, high speed and high radiation resistance. A large number of polytypes of SiC makes it possible to create heteropolytype structures (Lebedev et al., 2001, 2002a, 2005) to form a defect-free, near-perfect contacts with unusual electronic properties (Fissel et al., 2001; Lebedev et al., 2002b; Semenov et al., 2010). Diode structures have been established (Lebedev et al., 2002b), in which the value of uncompensated donors N_d-N_a was (1.7−2)×10^{17} см$^{-3}$ in the layer (n) 6H-SiC and acceptors $N_a-N_d \sim$ 3×10^{18} см$^{-3}$ in the layer (p) 3C-SiC. In the spectrum of the electroluminescence of diodes revealed two bands with maxima h$\nu_{max} \approx$ 2.9 eV (430 nm) and 2.3 eV (540 nm), close the band gaps of 6H-and 3C-SiC. Currently, using the methods of vacuum sublimation (Savkina et al., 2000), molecular beam epitaxy (Fissel et al., 1996), the epitaxial and heteropolytype layers based on the cubic 3C-SiC and two hexagonal 6H-SiC, 4H-SiC on substrates of SiC, are grown. By chemical vapor deposition (CVD) (Nishino et al., 2002) are grown heteroepitaxial layers of 3C-SiC on substrates of Si. At the temperatures below 1200°C there are conditions for the growth of both poly- and nanocrystalline SiC with different degrees of crystallinity and structure of the cubic polytype 3C-SiC. Such conditions were realized in the magnetron sputtering (Kerdiles et al., 2000; Sun et al., 1998), laser ablation (Spillman et al., 2000) and plasma deposition (Liao et al., 2005), plasma-enhanced chemical vapor deposition (George et al., 2002; Pajagopalan et al., 2005), molecular beam epitaxy (Fissel et al., 2000). At temperatures below 1500°C in the direct deposition of carbon and silicon ions with an energy of ~100 eV, the growth of nanocrystalline films with a consistent set of the polytypes 3C, 21R, 27R, 51R, 6H is possible (Semenov et al., 2008, 2009, 2010). Photoluminescence spectrum from the front surface of the nanocrystalline film

containing cubic 3C and rhombohedral 21R, has a band emission with three peaks at 2.65, 2.83, 2.997 eV (469, 439, 415 nm), the shoulder of 2.43 eV (511 nm) and a weak peak at 3.366 eV (369 nm) (Semenov et al., 2010).

Of particular interest is the synthesis of SiC layers in silicon by ion implantation (Lindner, 2003; Liangdeng et al., 2008; Kimura et al., 1982, 1984) due to the possibilities to obtain the films of a given thickness and composition, nanolayers of chemical compounds and multilayer structures, as well as the insulating layers in the manufacture of integrated circuits. Silicon structures with a hidden layer of silicon carbide can be used as a SOI-structure (silicon-on-insulator), which have advantages over structures with a hidden layer of SiO_2, obtained by the SIMOX (Separation by IMplantation of OXygen). Crystalline films of high-quality β-SiC on SiO_2 can be obtained by multiple ion implantation of C in Si and selective oxidation of the top layer of Si (Serre et al., 1999).

High-dose carbon implantation into silicon in combination with subsequent or in situ thermal annealing has been shown to be able to form polycrystalline or epitaxial cubic SiC (β-SiC) layers in silicon (Liangdeng et al., 2008; Kantor et al., 1997; Durupt et al., 1980; Calcagno et al., 1996). To create a SiC−Si heterojunctions were among the first used the method of ion implantation the authors of (Borders et al., 1971; Baranova et al., 1971), in which the synthesis of silicon carbide was carried out by implantation of $^{12}C^+$ ions (E = 200 кэВ, D = ~10^{17} см$^{-2}$ (Borders et al., 1971) or E = 40 кэВ, D > 10^{17} ион/см^2 (Baranova et al., 1971)) into a silicon substrate. From the position of the IR absorption band (700–725 cm^{-1}), reducing its half-width after annealing and displacement in the region at 800 cm^{-1}, corresponding to transverse optical phonons of SiC, it was found that the formation of crystalline SiC phase occurs in the temperature range near 850ºC (Borders et al., 1971) and 900°C (Baranova et al., 1971). Silicon carbide was identified using transverse optical phonon spectra in most of the above work on ion implantation, as well as in (Gerasimenko et al., 1974, Wong et al., 1998, Akimchenko et al., 1977a, 1980; Chen et al., 1999, Kimura et al., 1981). The detection of longitudinal optical vibrations of lattice atoms (LO phonons) and their changes during film annealing give additional information on the crystallization processes (Akimchenko et al., 1977b, 1979).

Difficulties associated with the problem of synthesis of a crystalline silicon carbide prevent the wide use of SiC in microelectronics. The Si-C mixture, after implantation of large doses of carbon, is assumed to be amorphous (Lindner , 2003; Liangdeng et al., 2008; Kimura et al., 1981). Carbon atom diffusion in the implanted layer is restricted by the strong Si-C bonds (Liangdeng et al., 2008). A negative influence of stable C- and C−Si-clusters (Yan et al., 2000, Chen et al., 2003; Kimura et al., 1982, 1984; Durupt et al., 1980, Calcagno et al., 1996; Borders et al., 1971) on the crystallization of SiC in the implanted silicon layers with different concentration of the implanted carbon, was found. Heat treatment up to 1200°C does not lead to complete disintegration of the clusters and the release of C and Si atoms to form the Si–C-bonds with tetrahedral orientation which is characteristic of the crystalline SiC phase (Khokhlov et al., 1987). However intensively developing area is the formation in SiO_2 by ion implantation of nanostructured systems with inclusions of nanocrystals and clusters of Si, SiC and C, providing the expense of size effects luminescence virtually the entire visible spectrum (Zhao et al., 1998; Tetelbaum et al., 2009; Perez-Rodrıguez et al., 2003; Gonzalez-Varona et al., 2000; Belov et al., 2010). This makes it necessary to study the mechanisms of formation of nanocrystals Si, SiC, carbon nanoclusters and amorphous SiC precipitates during the implantation and

annealing. It is of considerable interest to study the effect of the concentration component, nanoclusters, the phase composition of SiC films and their heat or plasma treatment on the crystallization processes and clustering, the size of nanocrystals and, consequently, the physical properties of the films.

A number of studies have shown that the implantation of ions with multiple different energies is the most suitable for obtaining a uniform layer of carbon and silicon atoms to form SiC (Liangdeng et al., 2008, Calcagno et al ., 1996, Srikanth et al., 1988, Rothemund&Fritzsche, 1974, Reeson et al., 1990, Lindner et al., 1996; Martin et al., 1990). By carefully selecting the values of implantation energy and corresponding doses of carbon ions, a rectangular carbon concentration profile can be achieved for the buried β-SiC layer using this approach.

Implantation of carbon ions at temperatures of silicon substrate well above room temperature by in-situ annealing helps to form SiC crystalline layers immediately during implantation or after annealing at lower temperatures (Durupt et al., 1980; Frangis et al., 1997; Edelman et al., 1976; Simon et al., 1996; Preckwinkel et al., 1996). High temperature of the substrate can be achieved also by using beams with high current density of carbon ions (Reeson et al., 1990; Alexandrov et al., 1986). Treatment of carbon implanted silicon layers by power ion (Liangdeng et al., 2008; Bayazitov et al., 2003), electron (Theodossiu et al., 1999) or laser (Bayazitov et al., 2003a, 2003b) beams like thermal annealing also leads to the formation of a polycrystalline β-SiC layer.

In this paper, the composition and structure of homogeneous SiC$_{1.4}$, SiC$_{0.95}$, SiC$_{0.7}$, SiC$_{0.4}$, SiC$_{0.12}$ and SiC$_{0.03}$ layers, received by multiple high-dose implantation of carbon ions with energies of 40, 20, 10, 5 and 3 keV are investigated. The influence of decay of carbon- and carbon-silicon clusters during thermal annealing or hydrogen glow discharge plasma processing on the formation of tetrahedral Si–C-bonds and crystallization processes in silicon layers with high and low concentrations of carbon, is studied.

2. Experimental

Single-crystal (100) silicon wafers of sizes 7×12×0.4 mm^3 with an electrical resistivity 4–5 Ω·cm were implanted by ^{12}C$^+$ ions with energies of 40, 20, 10, 5, and 3 keV at room temperature in vacuum reached by fully oil-free pumping. To prevent sample heating, the ion current density was kept below 4 μA/cm^2.

The SiC$_x$ films structure was investigated by X-ray diffraction using a narrow collimated (0.05×1.5 mm^2) monochromatic (CuK$_\alpha$) X-ray beam directed at an angle of 5° to the sample surface. The average crystallite size was estimated from the width of X-rays lines by Jones method. The surface of the layers was analyzed by Atomic force microscopy (JSPM 5200, Jeol, Japan) using AFM AC technique. The investigation of morphology and structure of the SiC$_x$ layers was carried out by transmission electron microscopy (JEM-100CX, JEOL, Japan). The IR transmission spectra were recorded in differential regime on double-beam infrared spectrometer UR-20 (400–5000 cm^{-1}). The spectra both at perpendicular incidence of infrared rays on the sample surface and at an angle of 73° with respect to the normal to the sample surface were measured. The composition of the layers was examined by Auger electron spectroscopy. The parameters were as follows: incident electron beam of diameter 1 μm, energy 10 keV, angle of incidence 45°, diameter of scanning region 300 μm, vacuum 1.33 ×10^{-8} Pa, angle of Ar$^+$ beam incidence 45°.

The glow discharge hydrogen plasma was generated at a pressure of 6.5 Pa with a capacitive coupled radio frequency (r.f.) power (27.12 MHz) of about 12.5 W. The temperature of processing did not exceed 100°C and it was measured by thermocouple. The processing time was 5 min.

3. Results and discussion

3.1 Depth profiles of multiple-energy implanted carbon in Si

To produce a rectangular profile of the distribution of carbon atoms in silicon five energies and doses have been chosen in such a way (Table 1) that the concentration ratio of C and Si atoms to a depth (up to ~120 nm) was equal to the values of N_C/N_{Si} = 1.0 , 0.8, 0.5, 0.3, 0.1 and 0.03. The calculated profiles N_C(Burenkov) are the sums of the distributions (Figs. 1 and 2), constructed for the chosen values of energies (E) and doses (D) of carbon ions using the values of the ion mean projective range, R_p(E), and the root-mean-square deviation, ΔR_p(E), (Table 1) and moment $S_k(E_o)$, according to Burenkov et al. (1985). On these figures are presented the calculated profiles N_C(Gibbons), which are the sums of Gaussian distributions constructed by using values of R_p(E) and ΔR_p(E) according to Gibbons et al. (1975) (LSS):

$$N(x) = \frac{D}{\Delta R_p (2\pi)^{1/2}} \exp[-\frac{(x - R_p)^2}{2\Delta R_p^2}], \tag{1}$$

where x is the distance from the surface.

Figs. 1 and 2 also show the experimental profiles N_C(20°C), N_C(1250°C) and N_O(1250°C), obtained by Auger electron spectroscopy, which show the concentration ratio of carbon and oxygen atoms (N_C/N_{Si} and N_O/N_{Si}) over the sample depth after implantation and annealing at 1250°C for 30 min in an argon atmosphere with low oxygen content. Fig. 1 shows that the average concentrations of carbon and oxygen were: a)N_C/N_{Si} = 1.4 and N_O/N_{Si} ≈ 2.6; b) N_C/N_{Si} = 0.95 and N_O/N_{Si} ≈ 2.33; c) N_C/N_{Si} = 0.7 and N_O/N_{Si} ≈ 3.0; and as follows from Fig. 2: a)N_C/N_{Si} = 0.4; b)N_C/N_{Si} = 0.12.

Thus, the average carbon concentration over the depth exceeded the corresponding calculated values (N_C/N_{Si} = 0.1; 0.3; 0.5; 0.8 and 1.0) and led to the formation of layers $SiC_{0.12}$, $SiC_{0.4}$, $SiC_{0.7}$, $SiC_{0.95}$ and $SiC_{1.4}$ (Table 2). The average value of the ratio of N_O/N_{Si} exceeded the stoichiometric value for SiO_2 (N_O/N_{Si} = 2), indicating on the saturation of the surface layer by oxygen. In high-temperature annealing a desorption of carbon atoms from the surface and an adsorption of oxygen atoms are occurred. There are clear interfaces $SiO_{3.0}$:$SiC_{0.7}$, $SiO_{2.33}$:$SiC_{0.95}$ and $SiO_{2.6}$:$SiC_{1.4}$ suggesting the interconnectedness of these processes. The mechanism of desorption of carbon may be associated with a diffusion process along the grain boundaries of counter flow of oxygen molecules O_2 into deep layer and molecules of CO and CO_2 from the layer toward the surface.

Penetration of oxygen deep into the implanted layer until the substrate was also shown in (Chen et al., 2003). The mechanism of instability of silicon carbide films during high-temperature annealing in the presence of oxygen is of special interest (Singh et al., 2002).

Process can occur in accordance with the expression $2SiC + 3O_2 \xrightarrow{950-1700°C} 2SiO_2 + 2CO$.

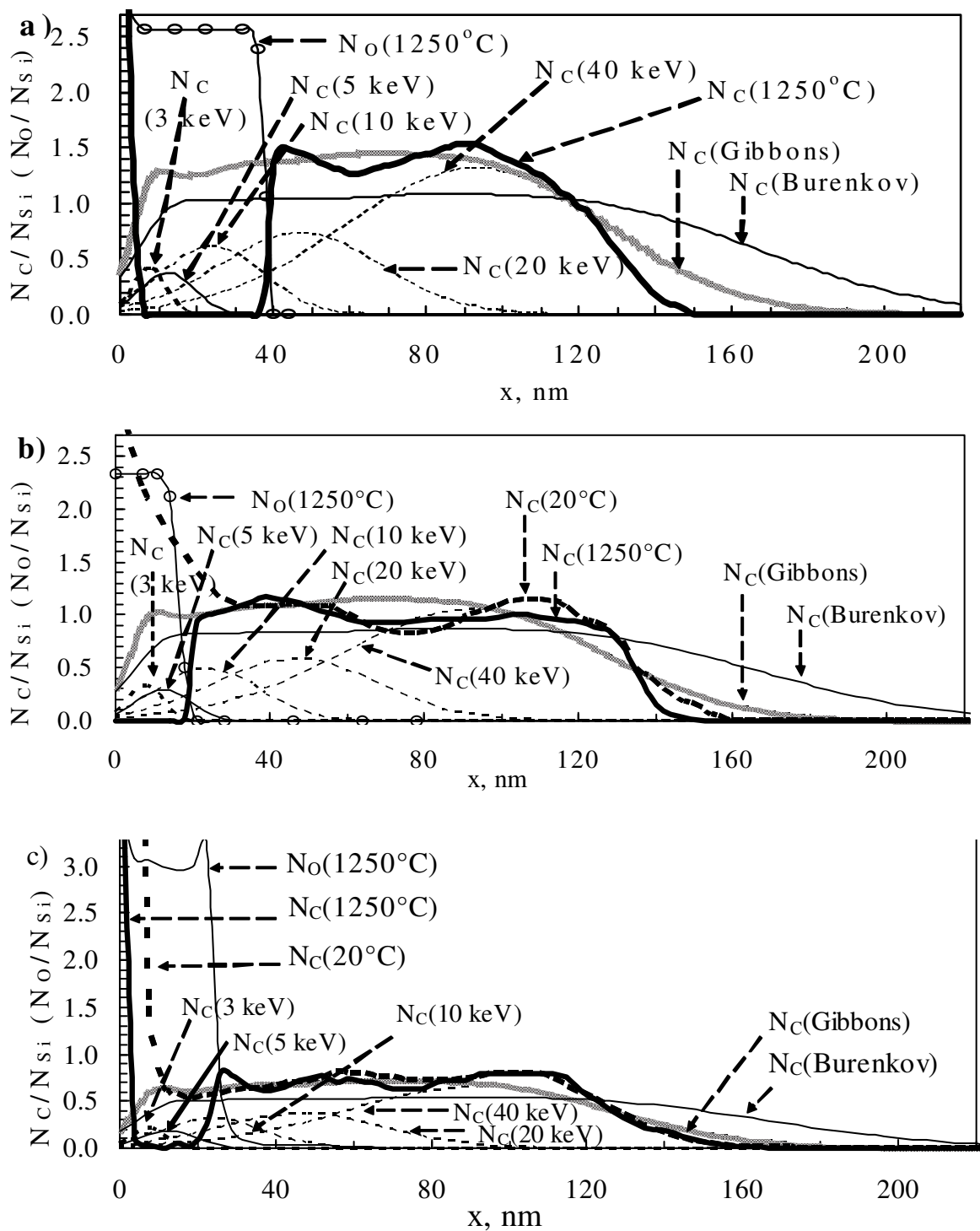Fig. 1. ^{12}C distribution profiles in Si produced by ion implantation (see table 1). (a) SiC$_{1.4}$; (b) SiC$_{0.95}$; (c) SiC$_{0.7}$. N$_C$(Burenkov) and N$_C$(Gibbons) are the profiles calculated according to Burenkov et al. (1985) and Gibbons et al. (1975), respectively, where N$_C$(Gibbons) = N$_C$(40 keV) + N$_C$(20 keV) + N$_C$(10 keV) + N$_C$(5 keV) + N$_C$(3 keV). N$_C$(20^{0}C), N$_C$(1250^{0}C) and N$_O$(1250^{0}C) are the Auger profiles of carbon and oxygen, respectively, in a layer after high-dose implantation and annealing at T = 1250°C for 30 min.

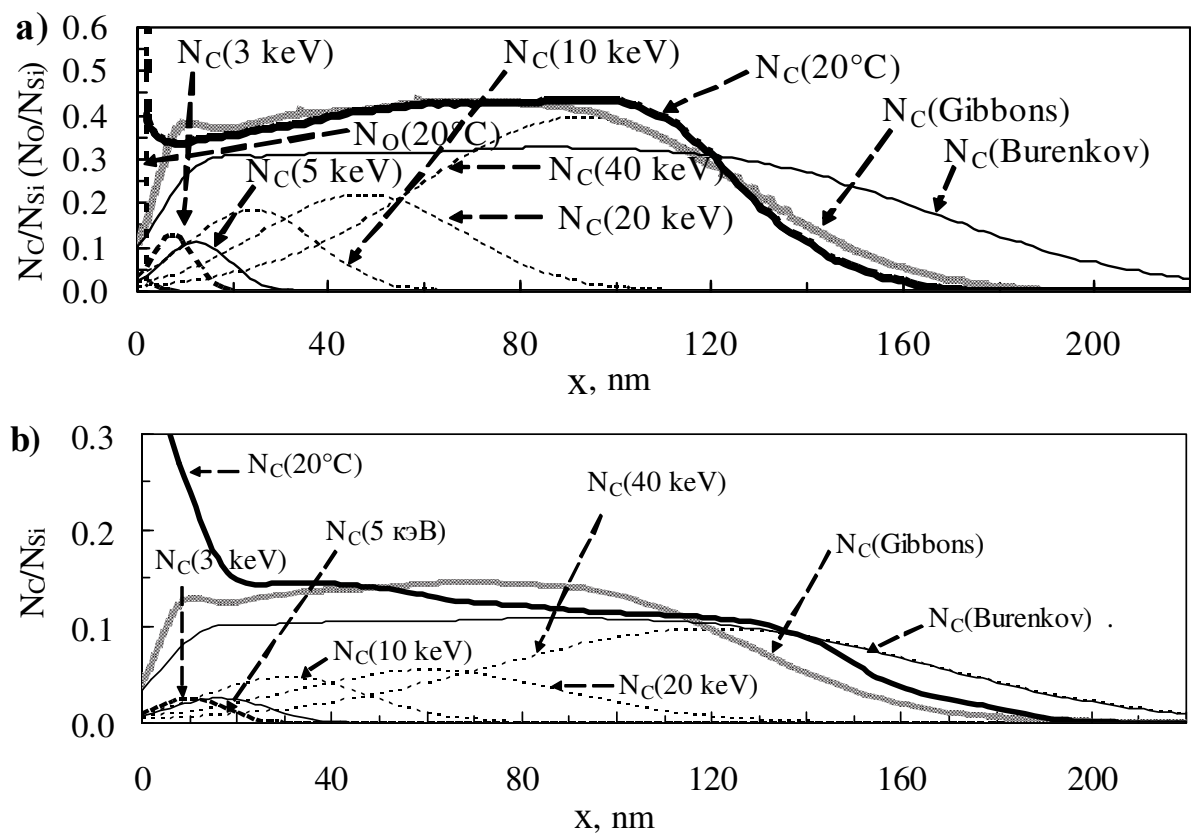Fig. 2. ^{12}C distribution profiles in Si produced by ion implantation (see table 1). (a) $SiC_{0.4}$; (b) $SiC_{0.12}$. N_C(Burenkov) and N_C(Gibbons) are the profiles calculated according to Burenkov et al. (1985) and Gibbons et al. (1975), respectively, where N_C(Gibbons) = N_C(40 keV) + N_C(20 keV) + N_C(10 keV) + N_C(5 keV) + N_C(3 keV). N_C(20^{0}C) and N_O(20^{0}C) are the Auger profiles of carbon and oxygen, respectively, in a layer after high-dose implantation.

E, keV		40	20	10	5	3
$D(SiC_{1.0})$, 10^{17} cm^{-2}		5.60	1.92	0.990	0.330	0.230
$D(SiC_{0.8})$, 10^{17} cm^{-2}		4.48	1.54	0.792	0.264	0.184
$D(SiC_{0.5})$, 10^{17} cm^{-2}		2.80	0.96	0.495	0.165	0.115
$D(SiC_{0.3})$, 10^{17} cm^{-2}		1.68	0.576	0.297	0.099	0.069
$D(SiC_{0.1})$, 10^{17} cm^{-2}		0.56	0.192	0.099	0.033	0.023
$D(SiC_{0.03})$, 10^{17} cm^{-2}		0.168	0.058	0.030	0.010	0.007
N_C(Burenkov) profile (Burenkov et al., 1985)	$R_p(E)$. nm	120.4	60.0	30.3	16.1	10.5
	$\Delta R_p(E)$. nm	46.0	28.3	16.9	10.2	7.2
N_C(Gibbons) profile (Gibbons et al., 1975)	$R_p(E)$. nm	93.0	47.0	24.0	12.3	7.5
	$\Delta R_p(E)$. nm	34.0	21.0	13.0	7.00	4.3

Table 1. Values of energy, E, dose, D, projected range, $Rp(E)$, and straggling, $\Delta Rp(E)$, for ^{12}C$^+$ ions in Si, used for constructing a rectangular distribution profile

In (Mandal et al., 2001) reported 100% conversion of SiC into SiO$_2$ in accordance with the expression of SiC + O$_2$ = SiO$_2$ + CO/CO$_2$.

In the case of high concentrations of carbon (SiC$_{1.4}$, SiC$_{0.95}$, SiC$_{0.7}$ and SiC$_{0.4}$) the experimentally obtained profiles of the carbon atoms were almost rectangular (Figs. 1 and 2) and close in concentration value to the calculated concentration profile according Gibbons et al. (1975), while for layers with low carbon concentration SiC$_{0.12}$ is closer to the calculated profile according Burenkov et al. (1985) (Fig. 2). Factors contributing to the excess concentration of carbon in the surface silicon layer in comparison with the calculated values by (Burenkov et al., 1985) at high-dose ^{12}C ion implantation can be considered sputtering the surface in conjunction with a decrease in the values of Rp due to the presence of strong Si-C- and C-clusters, double and triple Si–C- and C–C-bonds.

Depth range, nm	40–110	20–120	25–120	10–120	20–120
SiC$_x$ (Burenkov)	SiC$_{1.0}$	SiC$_{0.8}$	SiC$_{0.5}$	SiC$_{0.3}$	SiC$_{0.1}$
SiC$_x$ (Gibbons)	SiC$_{1.38}$	SiC$_{1.06}$	SiC$_{0.67}$	SiC$_{0.40}$	SiC$_{0.13}$
SiC$_x$ (AES)	SiC$_{1.4}$	SiC$_{0.95}$	SiC$_{0.7}$	SiC$_{0.4}$	SiC$_{0.12}$

Table 2. Average values of carbon concentration x = N_C/N_{Si} in the SiC$_x$ layers calculated according Burenkov et al. (1985) and Gibbons et al. (1975) and experimentally obtained by Auger electron spectroscopy

3.2 Investigation of the structure by electron microscopy

By transmission electron microscopy structural features of the SiC$_{1.4}$, SiC$_{0.95}$ and SiC$_{0.7}$ films, formed in the surface layer of single crystal Si wafers using multiple ion implantation, after annealing at 1200°C for 30 minutes were investigated. Figure 3 schematically shows a section of the objects. The investigated area can be divided into three sections: section 1 consists of a layer SiC$_x$; section 2 includes a [transition layer "Si-SiC$_x$" + layer SiC$_x$]; section 3 is a three-layer structure [layer-Si + transition layer "Si-SiCx "+ layer SiCx].
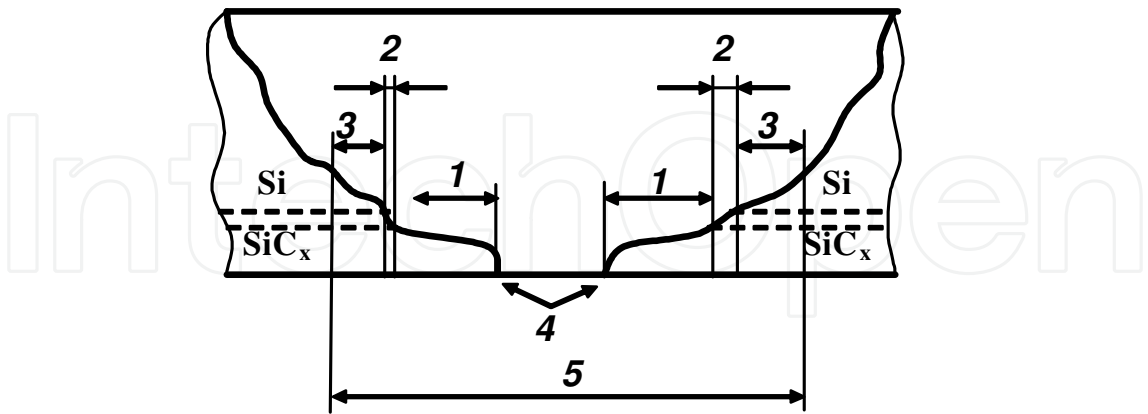

Fig. 3. Schematic cross section of the sample under study: (1) SiC$_x$ regions, (2) regions of an intermediate Si-SiC$_x$ layer, (3) double-diffraction regions, (4) a through hole, and (5) the area to be analyzed by transmission electron microscopy.

The layers SiC$_{1.4}$, SiC$_{0.95}$ and SiC$_{0.7}$ are solid, homogeneous, fine polycrystalline films (Figs. 4a-c, 5a, b and 6a, b, light areas, respectively). Some electron diffraction patterns contain superimposed point (c-Si) and ring (SiC) electron diffraction patterns (Fig.4b, c, 5b and 6b).

These patterns were recorded from areas 3 where the objects were presented together with single- and polycrystalline structures (for example Si + SiC$_{1.4}$). In Figs. 4b, 5b and 6b the microstructure of sections 1 (light area), 2 (intermediate region) and 3 (dark area) are shown.
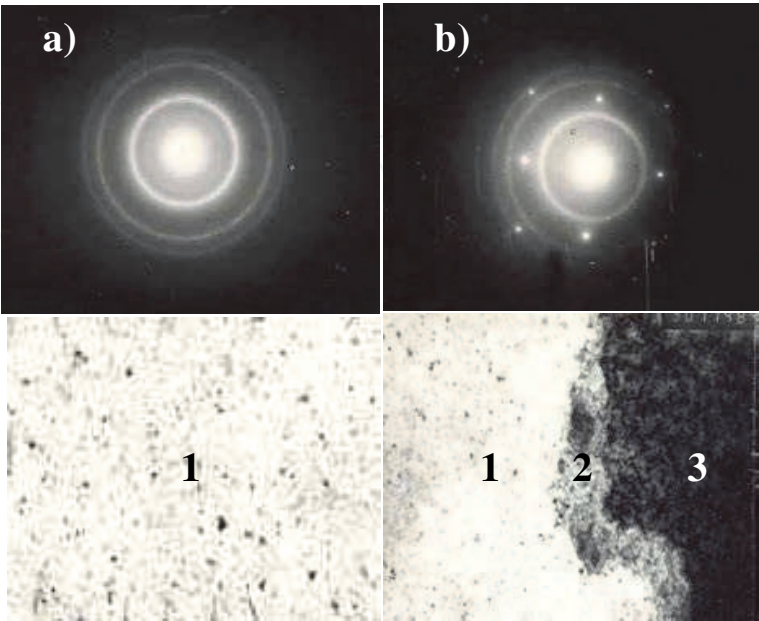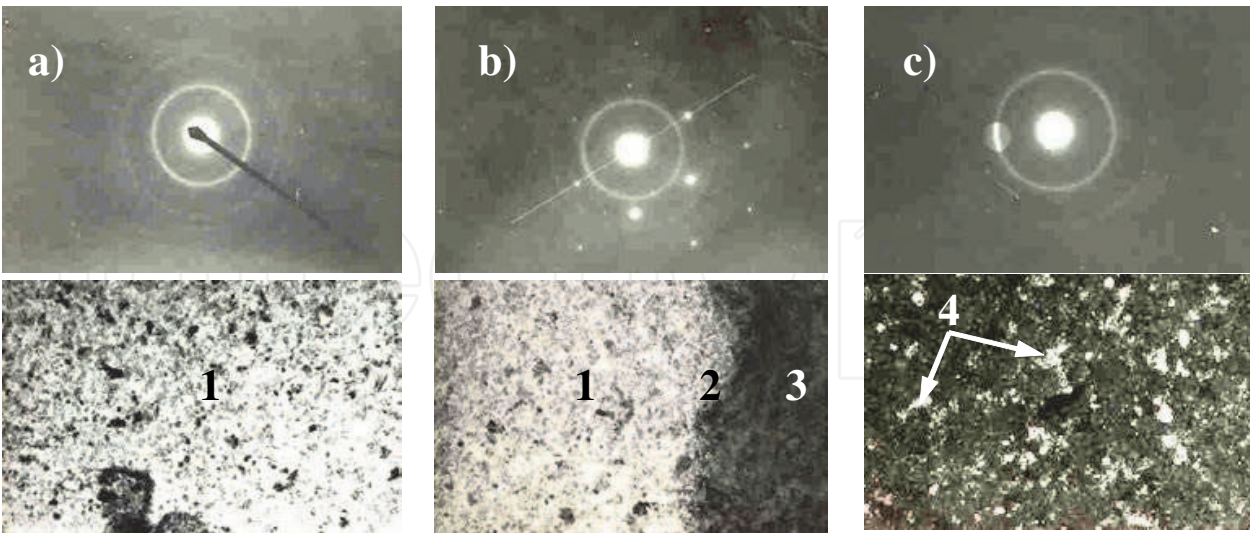

Fig. 4. Electron diffraction patterns and microstructure (×50000) of the SiC$_{1.4}$ layer after annealing at temperature 1200^{0}C for 30 min: rings – SiC, point reflections – Si, bright regions – SiC$_{1.4}$ layer, dark regions – c-Si. a) SiC$_{1.4}$ region; b) SiC$_{1.4}$ regions + intermediate Si– SiC$_{1.4}$ layer + c-Si: (*1*) SiC$_{1.4}$ regions, (*2*) regions of an intermediate Si– SiC$_{1.4}$ layer, (*3*) double-diffraction regions.

Fig. 5. Electron diffraction patterns and microstructure (×50000) of the SiC$_{0.95}$ layer after annealing at temperature 1200^{0}C for 30 min: rings – SiC, point reflections – Si, bright regions – SiC$_{0.95}$ layer, dark regions – c-Si. a) SiC$_{0.95}$ region; b) SiC$_{0.95}$ regions + intermediate Si–SiC$_{0.95}$ layer + c-Si, c) SiC crystallites in dark-field image regime: (*1*) SiC$_{0.95}$ regions, (*2*) regions of an intermediate Si–SiC$_{0.95}$ layer, (*3*) double-diffraction regions, (*4*) SiC crystallites.
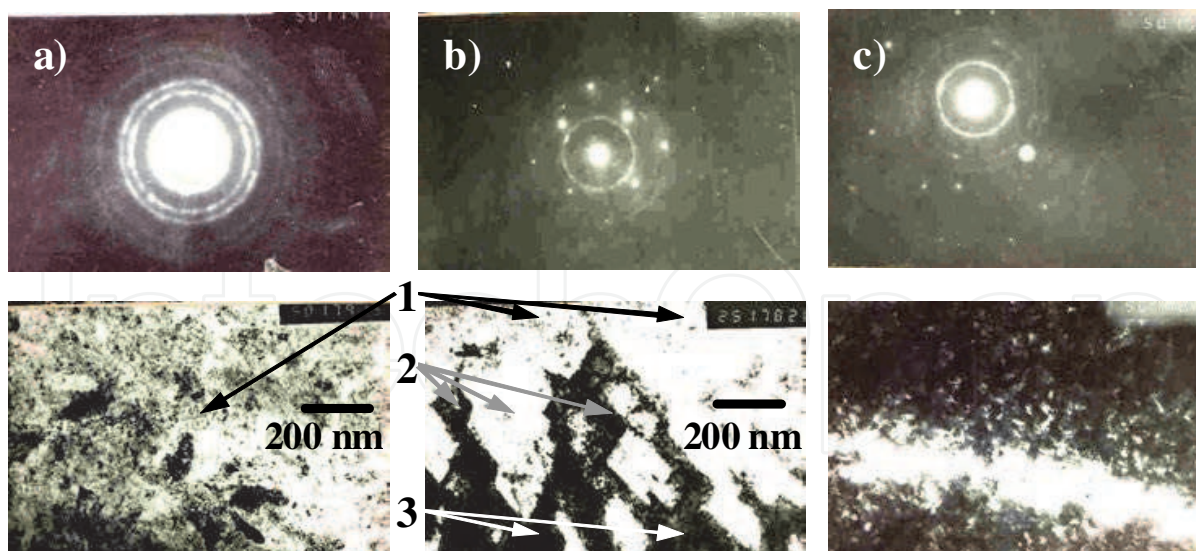
Fig. 6. Electron diffraction patterns and microstructure (×50000) of the SiC$_{0.7}$ layer after annealing at temperature 1200^{0}C for 30 min: rings – SiC, point reflections – Si, bright regions – SiC$_{0.7}$ layer, dark regions – c-Si. a) SiC$_{0.7}$ region; b) SiC$_{0.7}$ regions + intermediate Si–SiC$_{0.7}$ layer + c-Si, c) SiC crystallites in dark-field image regime: (*1*) SiC$_{0.7}$ regions, (*2*) regions of an intermediate Si–SiC$_{0.7}$ layer, (*3*) double-diffraction regions

The value of D·d of device, calculated from the point patterns of the silicon lattice, was equal D·d = (3.53±0.01) nm·mm. The diameters D of the most intensive rings of SiC$_{1.4}$ pattern were 10.4, 14.0, 22.9 and 26.9 mm, corresponding to the (002) plane of graphite (d = 0.338 nm) and silicon carbide β-SiC(111), β-SiC(220), β-SiC(311) (Fig. 4), respectively. The absence of some rings on the patterns is caused by their weak intensity. The diameters of the most intensive rings of SiC$_{0.95}$ were also 14.0, 22.9 and 26.9 mm and correspond to β-SiC(111), β-SiC(220), β-SiC(311) (Fig. 5). The diameters of rings of SiC$_{0.7}$ diffraction pattern were 14.0, 22.9, 26.9, 28.0, 35.3, 39.7 mm (Fig. 6) and agree well with the calculated values of the diameters of 1, 3, 4, 5, 7 and 9 of the silicon carbide rings, corresponding to a system of planes β-SiC(111), β-SiC(220), β-SiC(311), β-SiC(222), β-SiC(331), β-SiC(422), (d = 0.2518 nm, 0.1542 nm, 0.1311 nm, 0.1259 nm, 0.1000 nm, 0.0890 nm, respectively). Graphite rings in the electron diffraction patterns of SiC$_{0.7}$ and SiC$_{0.95}$ are not explicitly observed, which may be due to the absence of excess carbon.

In dark-field image regime the individual grains are visible as bright light spots. For a layer SiC$_{0.95}$ (Fig. 5c), as well as for the layer SiC$_{1.4}$, the presence of small and large grains of size from 10 to 80 nm was observed. The crystallites have various shapes - globular or plate-like. For a layer SiC$_{0.7}$ (Fig. 6c) crystallites were globular, needle or plate-like and had sizes from 10 to 400 nm after annealing at 1200°C. Small crystallites have a globular shape. These data differ from the X-ray diffraction data which was 5−10 nm (Akimchenko et al., 1977, 1980, Calcagno et al., 1996). It should be noted that by X-ray diffraction the average crystallite size was determined. In the layer SiC$_{0.7}$ due to the high concentration of carbon atoms one can expect a large number of stable clusters that hinder the crystallization process. In this case a significant prevalence of nanocrystals of a few nanometers sizes can be expected that are making a major contribution to the value of the average grain size. Small nanocrystals should give a reflection of the size in hundredths and tenths of a millimeter on the pattern, it is difficult to distinguish them and they are observed as a bright diffuse background between the larger crystallites (Fig. 6c).

Transition layer with a lower concentration of carbon between the Si substrate and $SiC_{0.7}$ is not uniform. It can be assumed that excess silicon atoms that are between the large SiC grains, in the process of recrystallization are combined with the substrate, forming a sawtooth SiC–Si structure (Fig. 6b).

3.3 Investigation of the structure by X-ray diffraction

After annealing of the $SiC_{1.4}$ layer in vacuum 10^{-4} Pa at temperatures 1200 and 1400°C in the X-ray diffraction patterns the intensive lines of polycrystalline silicon carbide are observed (Fig. 7a, b). There are also weak lines of polycrystalline silicon, apparently, from the transition layer "Si–$SiC_{1.4}$", where presents excess silicon, forming in the annealing process the Si crystallites. The integrated intensity of SiC lines after annealing at 1400°C was significantly lower than after annealing at 1200°C. This may occur because of the disintegration of silicon carbide and desorption of carbon from the layer at temperatures above 950°C (see section 3.1).   The decrease in phase volume of nanocrystalline SiC at temperatures above 1200°C can also occur due to evaporation of silicon in a vacuum, the melting point (1423°C) of which is less than the sublimation temperature of carbon (Semenov et al., 2009).
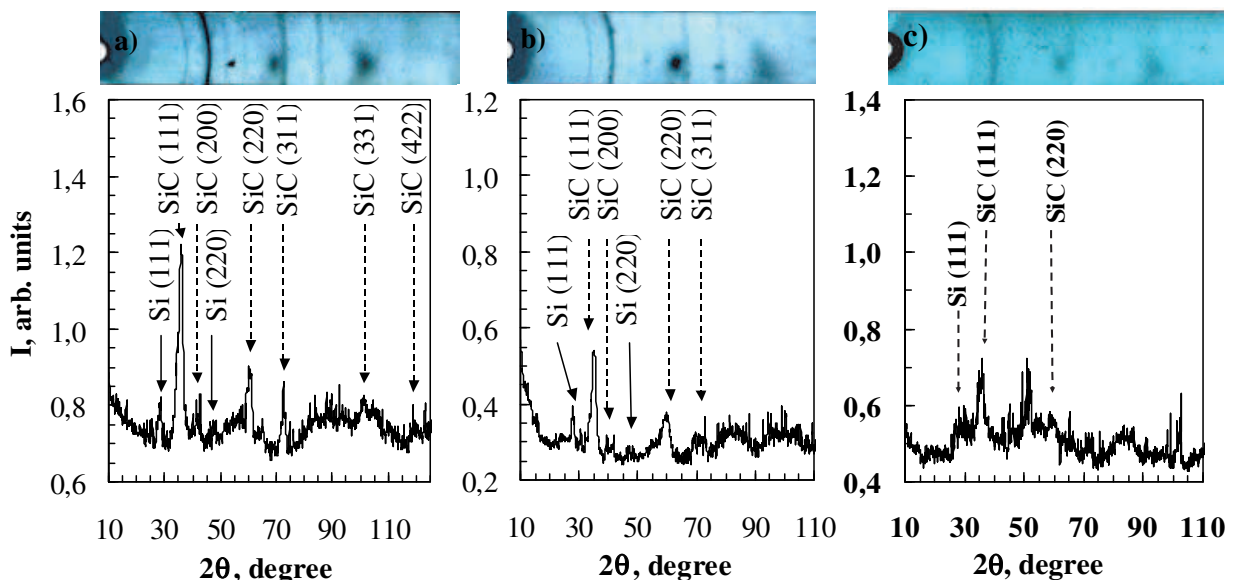

Fig. 7. X-ray diffraction patterns of the $SiC_{1.4}$ layer annealed for 30 min at (a) 1200 °C, (b) 1400°C, (c) after annealing at 1400°C and processing by glow discharge hydrogen plasma for 5 min.

An absence of SiC crystallites and the corresponding X-ray lines at high annealing temperatures 900–1100°C indicates a low ability of atoms to diffusion in the layer $SiC_{1.4}$. This may be caused by high concentrations of stable double and triple bonds like Si=C, Si≡C, C=C, C≡C, Si=Si, Si≡Si and strong clusters that prevent the diffusion of atoms in the layer and are decomposed at temperatures of 1200°C and above. An attempt was made to use processing by the hydrogen glow discharge plasma for the modification of the structural properties of the SiC_x films. For this purpose, the $SiC_{1.4}$ layer annealed at 1400°C was treated by the hydrogen glow discharge plasma (27.12 MHz, 12.5 W, 6.5 Pa, 100°C, 5 min).

After treatment by H-plasma is not taken place the complete destruction of the SiC crystallites (Fig. 7c). However, the intensity of X-ray lines of SiC decreased in comparison with the corresponding lines on the diffraction pattern before treatment (Fig. 7b). This demonstrates the

destructive effect of plasma on the structure of the β-SiC crystallites, although the capacity of plasma was only 12,5 W, and SiC on the hardness scale, according to Knoop holds a high place (SiC, 2480) after diamond (C, 7000), boron carbide (B4C , 2750), and aluminum boride (AlB, 2500). In addition, the processing by H-plasma for 5 minutes led to complete disappearance of the lines Si(111) and Si(220), reflected by the crystallites of silicon in the transition layer "film-substrate" ("SiC-Si"). It follows that the effect of hydrogen plasma propagates on the entire depth of the implanted layer (200 nm) and involves a intensive penetration of hydrogen ions through the solid film. Thus, the characteristics of the hydrogen glow discharge plasma and treatment (27.12 MHz, 12.5 W, 6.5 Pa, 100°C, 5 min) were sufficient to break the Si-Si and Si-C tetrahedral bonds and can be used to decay the stable carbon and carbon-silicon clusters.

Immediately after implantation and annealing of the SiC$_{0.95}$ layer at 1100°C and below (Fig. 8a) on the diffraction patterns not seen any lines of polycrystalline phases. A weak line of β-SiC(111) after annealing at 1150°C is observed, which becomes more pronounced after annealing at 1250°C (Fig. 8b). In contrast to the layers SiC$_{1.4}$ and SiC$_{0.95}$, the diffraction pattern of the SiC$_{0.7}$ layer (Fig. 8c) demonstrates the presence of β-SiC(111) line and weak Si (111) line after annealing at relatively low temperature of 1000°C for 30 minutes, due to the decrease of carbon concentration and, consequently, the concentration of stable carbon clusters. Annealing at 1100°C led to an increase in the intensity of the β-SiC(111) and Si(111) lines (Fig. 8d) and to an appearance of β-SiC(200), β-SiC(220), β-SiC(311) и Si(220) lines, which indicates an improvement in the crystallite structure. Line intensity from the SiC$_{0.7}$ layer shows a preferred content of polycrystalline β-SiC phase after annealing in comparison with the phase content of poly-Si, which is caused by a relatively high concentration of carbon. The average crystallite size of β-SiC and Si was about 3 – 7 nm in the planes: β-SiC(111) ~ 3 nm, β-SiC(220) ~ 6.5 nm, Si(111) ~ 4.5 nm.
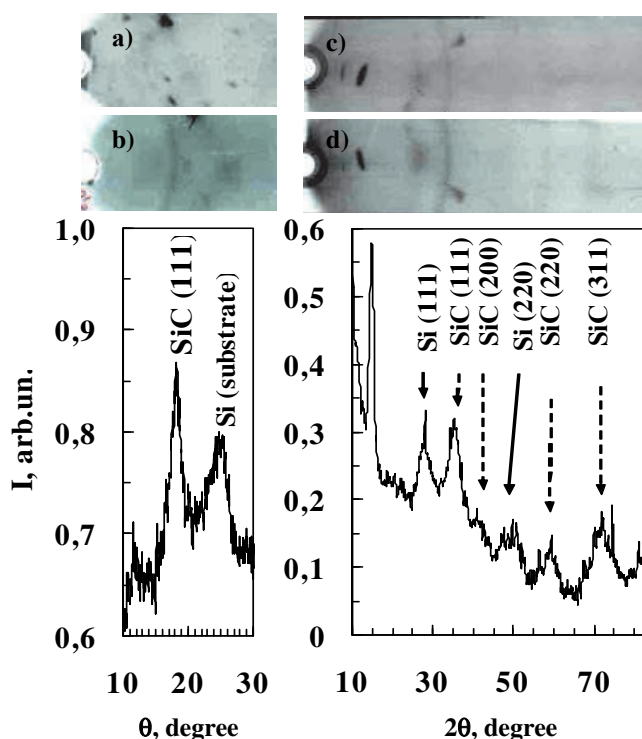

Fig. 8. X-ray diffraction patterns of the SiC$_{0.95}$ layer annealed at (a) 1100°C, (b) 1250°C and of the SiC$_{0.7}$ layer annealed at (c) 1000°C, (d) 1100°C , for 30 min obtained using X-ray chambers RKD (a, b) and RKU-114M1 (c, d). Intensity curves correspond to X-ray patterns (b, d).

In the layer $SiC_{0.4}$ the presence of polycrystalline phases of SiC and Si after implantation and annealing at 1000, 1100 and 1250°C are revealed. High intensity peaks of SiC after annealing at 1100°C (Fig. 9a) indicates on intensive process of crystallization of β-SiC due to lower content of stable clusters in comparison with the layers $SiC_{1.4}$, $SiC_{0.95}$ and $SiC_{0.7}$. High amplitude of β-SiC peaks after annealing at 1250°C confirms this assertion. In diffraction pattern of $SiC_{0.12}$ layer after implantation a broad diffuse line of amorphous silicon Si(111) ($\theta = 14.3°$) is observed (Fig.10a). After annealing at 800°C a narrowing of this line, at 900°C - a sharp narrowing of the line Si(111) and the appearance of Si(220) and Si(311) lines of polycrystalline Si phase, as well as two weak lines of β-SiC, at 1250°C - a decrease of the integrated intensity of Si lines, are observed.
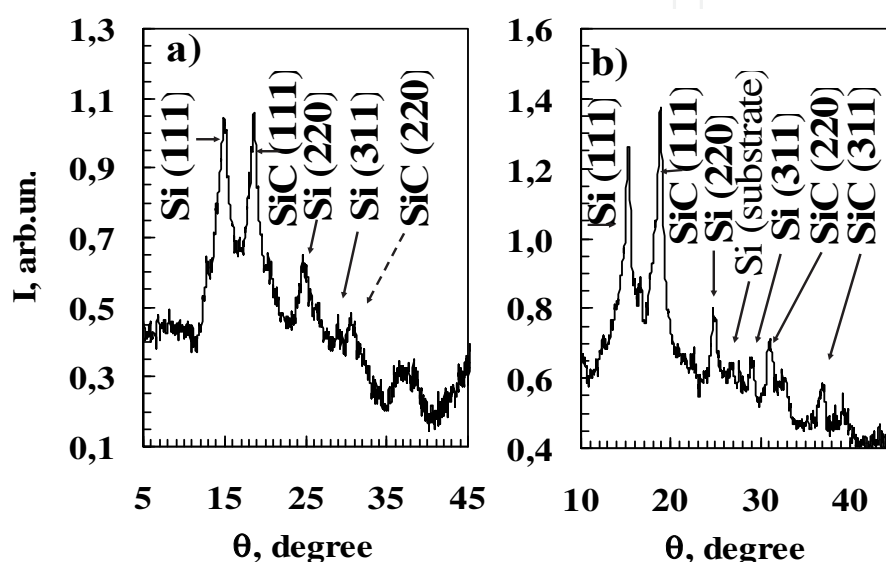

Fig. 9. X-ray diffraction patterns of the $SiC_{0.4}$ layer annealed for 30 min at (a) 1100°C and (b) 1250°C.

The implantation of carbon causes the formation of weakly ordered set of randomly oriented Si regions of size ~1.5 nm. Temperature dependence of the average crystallite size Si (Fig. 11a, curve 1) and SiC (curve 2) in plane (111) shows that at low temperatures the curve 1 is characterized by slow growth in the size of weakly ordered Si nanocrystals. Their transformation into well ordered Si crystallites at 800°C is taken place. Average size of Si crystallites is 47 nm after annealing at 1250°C. The formation of β-SiC crystallites prevent a complete recrystallization of layer at this temperature.

The integrated intensity curve of Si(111) line, which is proportional to the phase volume, has three sections in the temperature ranges of 20– 800°C, 800−900°C and 900−1250°C (Fig. 11b). In the range of 20-800°C I_{int} decreases, indicating a decrease in the total volume of nanocrystals Si, although their sizes increase up to 2.2 nm. The growth of weak ordered Si crystallites is accompanied by the displacement of carbon atoms in the surrounding space, which no longer contribute to the intensity of the Si (111) line due to increased concentration of carbon. In addition, there is recrystallization of silicon near the substrate. It is assumed that, after annealing at 800°C (Figs. 11b and 12) approximately $k_{800} \approx [I_{int}(800°C)/I_{int}(20°C)] \times 100\% = 72\%$ of silicon atoms in the layer is incorporated into crystallites of Si. The remaining atoms of Si (28%) are in an amorphous mixture of Si and C atoms, or reunited with the substrate.
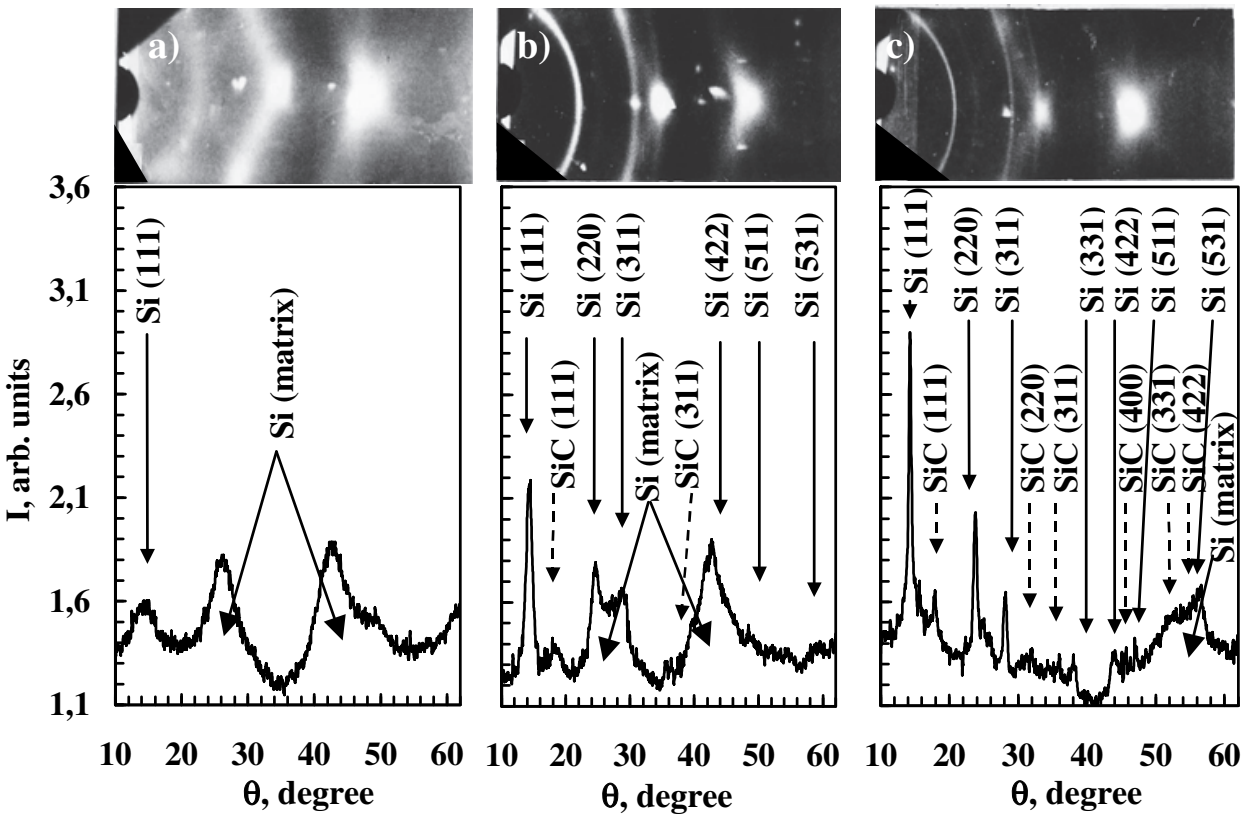
Fig. 10. X-ray diffraction patterns of the SiC$_{0.12}$ layer (a) before and after annealing for 30 min at (b) 1100ºC and (c) 1250°C.
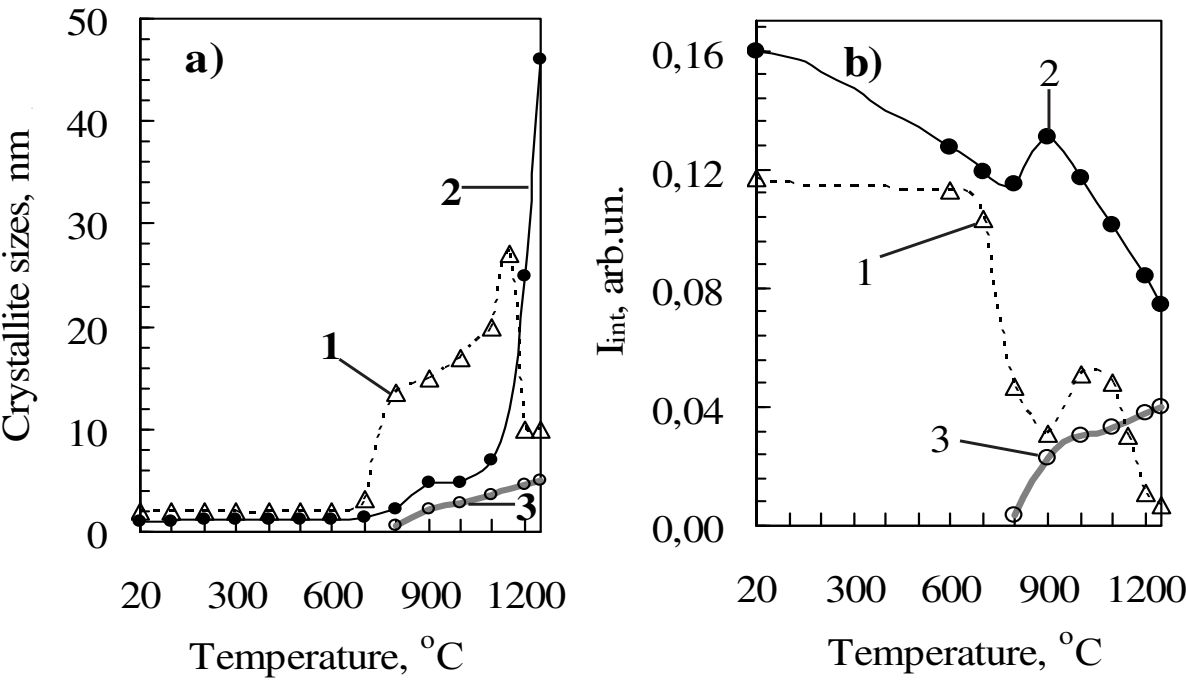

Fig. 11. Average sizes (a) of Si and SiC crystallites in the (111) plane and (b) the integrated intensities of the Si(111) and SiC(111) lines after implantation of carbon ions in silicon and annealing. 1 – Si (for layer SiC$_{0.03}$), 2 – Si (for layer SiC$_{0.12}$), 3 – SiC (for layer SiC$_{0.12}$).

Fig. 12 schematically shows the variation of the structure of the layer, its phase composition and phase volume, as well as the average grain size as a function of annealing temperature (a) and scheme of Si and SiC crystallite formation in this layer (b). The diagram is based on the curves in Fig. 11a, b for $SiC_{0.12}$. Regions "amorphous Si-C mixture" and "c-Si" are formed adhering to the relation: "amorphous Si-C mixture" + "c-Si" = 100% − ("poly-SiC" + "poly-Si"+"amorphous -Si").
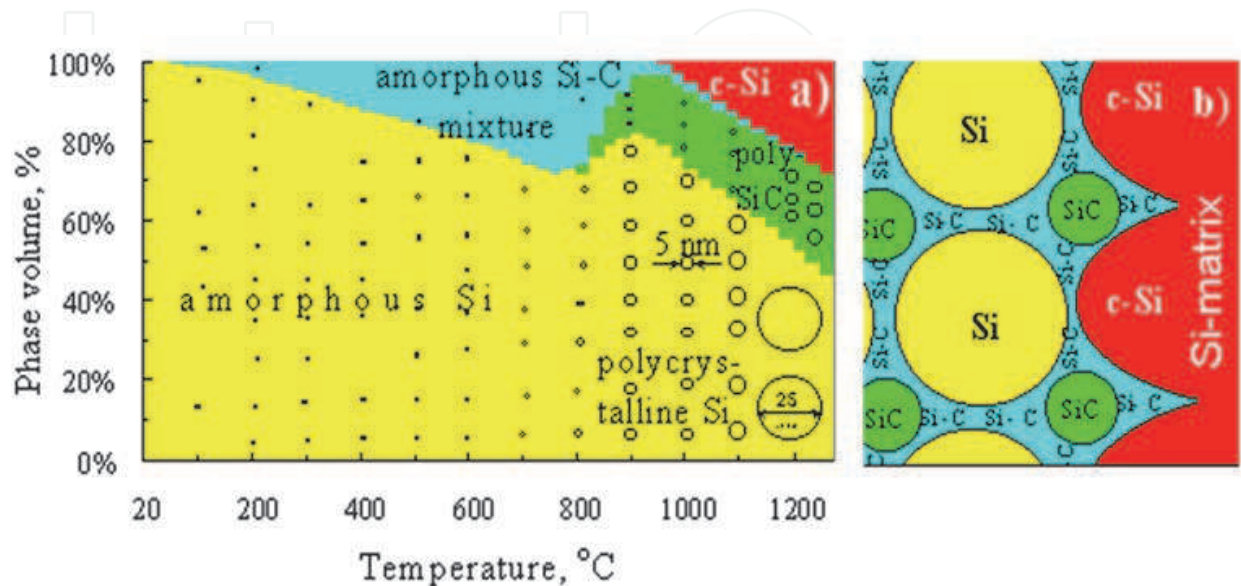

Fig. 12. Crystallization of the $SiC_{0.12}$ layer: (a) the phase volumes at various annealing temperatures and (b) the formation of crystalline Si and SiC crystallites in the temperature range 900−1000°C.

In the range of 800−900°C the increase in both size crystallites Si (from 2.2 to 4.7 nm) and the volume of polycrystalline phase of Si (Fig. 11a and 12) is observed. This is due to the formation of SiC crystallites at 900°C in the regions of carbon accumulation and the joining of excess silicon atoms to Si crystallites. So, k is increased: $k_{900} \approx 82\%$. This leads to a decrease in Si−C-mixture volume (Fig. 12). After annealing at 1000°C and 1250°C, an increase in the phase volume and crystallite sizes of β-SiC as well as a decrease in k due to recrystallization of regions near the Si substrate, are taken place: $k_{1000} \approx 73\%$ and $k_{1250} \approx 46\%$. Si crystallite sizes increased almost 10 times (up to 47 nm). Probably, there is destruction of defective silicon crystallites and the uniting of their atoms into crystallites with a perfect structure or with the substrate. As can be seen from the diagram, after annealing at 1200°C in the layer $SiC_{0.12}$ ~50% of silicon atoms are incorporated into Si crystallites with an average size of 25 nm, 25% of Si atoms are included into β-SiC crystallite with size of 5 nm and 25% are joined with Si substrate. Since the unit cell volume for Si is twice more than the cell volume for SiC, the volume of the surface layer of Si after implantation and annealing of carbon should not change appreciably, and the above relations can be regarded as a volume ratio of phases.
During annealing at 1400°C there is the destruction of most of the silicon crystallites and connection of their atoms to the substrate. The intensity of the lines Si was significantly lower than the intensities of β-SiC lines (Fig. 13). It is assumed that recrystallized Si layer with ingrained in him crystallites of β-SiC and Si on a silicon substrate was obtained.
During a growth of the crystallite size is manifested basic thermodynamic law: in an isolated system, the processes occurring with increasing free energy, is prohibited. Combining the

two grains is taken place, if it is accompanied by a gain in energy which is greater than its costs for the destruction of the crystallites. In this case, the redistribution of atoms with a change in chemical bond lengths and angles between them is taken place, in order to select a more favorable energy state, which is the states with tetrahedral oriented bonds, characteristic of crystalline phases of Si and SiC.
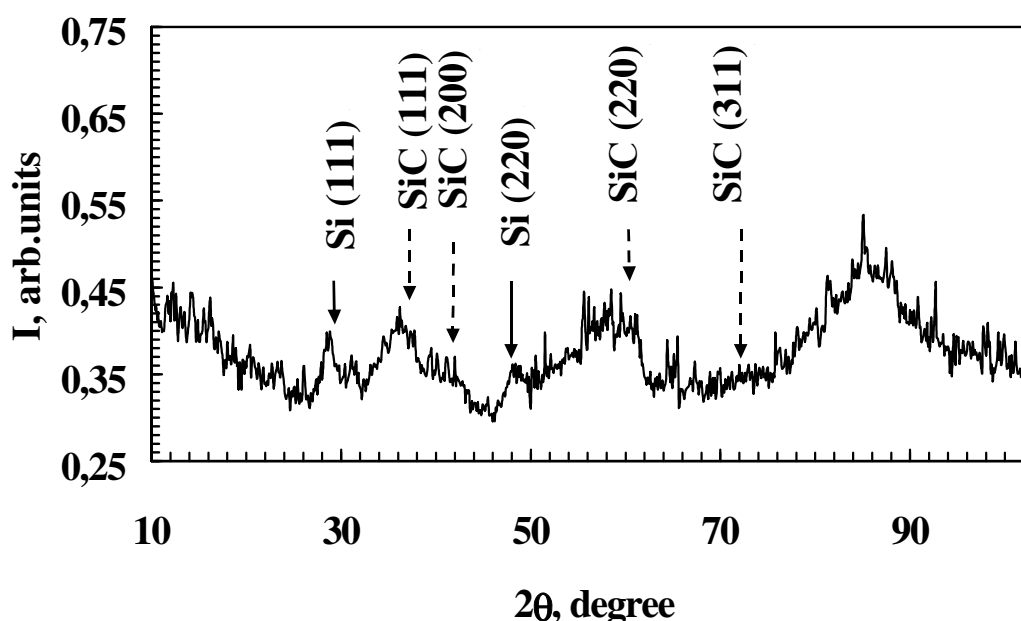

Fig. 13. X-ray diffraction pattern of the SiC$_{0.12}$ layer after annealing at 1400°C for 30 min.

The X-ray diffraction results are in accordance with the data of Auger electron spectroscopy, whereby the concentration of carbon atoms in a layer is N_C/N_{Si} = 0.12/1 (Fig. 2). Then the maximum possible ratio of atoms, forming part of SiC and Si, will be: N_{SiC}/N_{Si} = 0.24/0.88 = 0.27. As seen in Figure 11b, the maximum quantity of poly-SiC, obtained at 1250°C, was I_{int}(SiC) = 0.040, and poly-Si was I_{int}(Si) = 0.131 at 900°C, i.e., I_{int}(SiC)/I_{int}(Si) = 0.040/0.131 = 0.30, which is comparable with the data of Auger electron spectroscopy.

Similar features are observed for a layer with a lower carbon concentration SiC$_{0.03}$. Immediately after the implantation the same broad diffuse line of amorphous silicon Si(111) at θ = 14.3° is observed (Fig. 14). Increase of annealing temperature above 800°C causes narrowing of this line, increasing the number and amplitude of the line intensity which reaches its maximum at 1100°C. However, in the X-ray diffraction patterns of SiC$_{0.03}$ layer no lines of polycrystalline silicon carbide in the whole temperature range are observed due to insufficient concentration of the carbon atoms to form a large number of SiC crystallites. Annealing at temperatures above 1100° C reduces the intensity of Si lines and results their disappearance after annealing at 1250°C due to recrystallization of the layer.

For comparison, in Table 3 the grain sizes of silicon and silicon carbide in plane (111) in layers Si(111) and β-SiC(111) are given. Dimensions of weakly ordered regions in SiC$_{0.03}$ layer, contributing to the intensity of the Si(111) line, exceed the same values for SiC$_{0.12}$. This is associated with a lower concentration of carbon and larger volume of Si regions with extremely low concentrations of carbon. At temperatures of 1200 and 1250°C a decrease in the average crystallite size up to 10 nm is observed, which is associated with the process of recrystallization near the substrate.
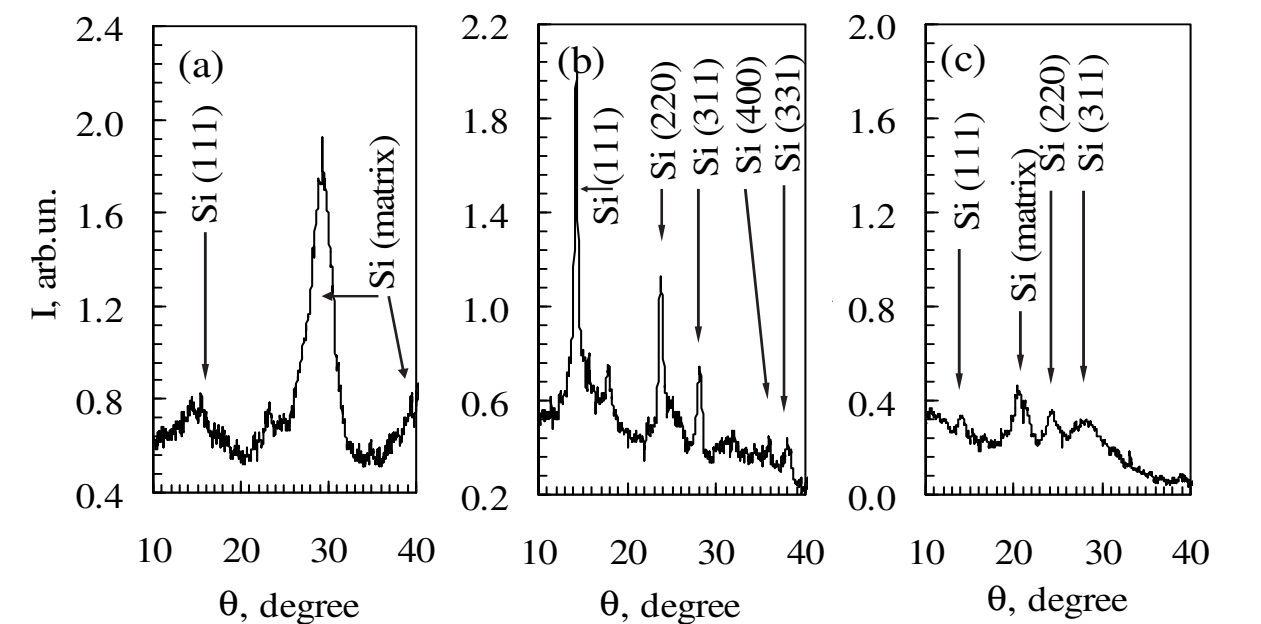
Fig. 14. X-ray diffraction of $SiC_{0.03}$ layer after implantation of carbon ions in Si (a) and annealing at 1100°C (b) and 1200°C (c) for 30 min.

Temperature (°C)	ε (nm)					
	$SiC_{0.03}$		$SiC_{0.12}$		$SiC_{0.4}$	
	Si	β-SiC	Si	β-SiC	Si	β-SiC
20	2	–	1.1	–	–	–
700	3	–	1.3	–	–	–
800	13	–	2	–	–	–
900	15	–	4.5	2		
1000	17	–	5	3	4	3
1100	20	–	7	3.5	4	3
1150	27	–	12	4		
1200	10	–	25	4.5		
1250	10	–	46	5	9	4.5

Table 3. Average size (ε) of Si- and β-SiC crystallites in SiC_x layers

Temperature dependences of the integrated intensity of Si(111) line (Fig. 15) for the $SiC_{0.03}$ and $SiC_{0.12}$ layers are similar in nature. A lower carbon concentration in $SiC_{0.03}$ layer results more intensive decrease in the phase volume of poly-Si at temperatures above 700°C due to more intensive recrystallization near the substrate. The value of k were: $k_{800} \approx 40\%$, $k_{900} \approx 27\%$, $k_{1000} \approx 44\%$, $k_{1100} \approx 41\%$, $k_{1250} \approx 6\%$. Growth of k up to 44% at 1000°C for $SiC_{0.03}$ layer due to accession of excess silicon atoms from the carbon-rich Si-C-mixture to the Si crystallite is taken place. For a layer $SiC_{0.12}$, that is observed at a temperature of 100°C below due to a higher concentration of carbon, therefore the carbon rich region is formed at lower temperatures and does not require significant movements of atoms. Annealing at 1250°C results in uniting of $SiC_{0.03}$ layer with single-crystal substrate ($K_{1250} \times 100\% = [0,007/0,116] \times 100\% = 6\%$) and the decrease in the average size of residual crystallites up to 10 nm.

3.4 Investigations by infrared spectroscopy

The influence of carbon concentration in the SiC$_x$ layers and annealing temperature on the parameters of the spectra of infrared spectroscopy was investigated. For this purpose, using two-beam infrared spectrometer UR-20 the IR transmission spectra of SiC$_{1.4}$, SiC$_{0.95}$, SiC$_{0.7}$, SiC$_{0.4}$, SiC$_{0.12}$ and SiC$_{0.03}$ layers before and after isochronous annealing in vacuum at temperature range 200−1400°C were measured (Figs. 16−21).
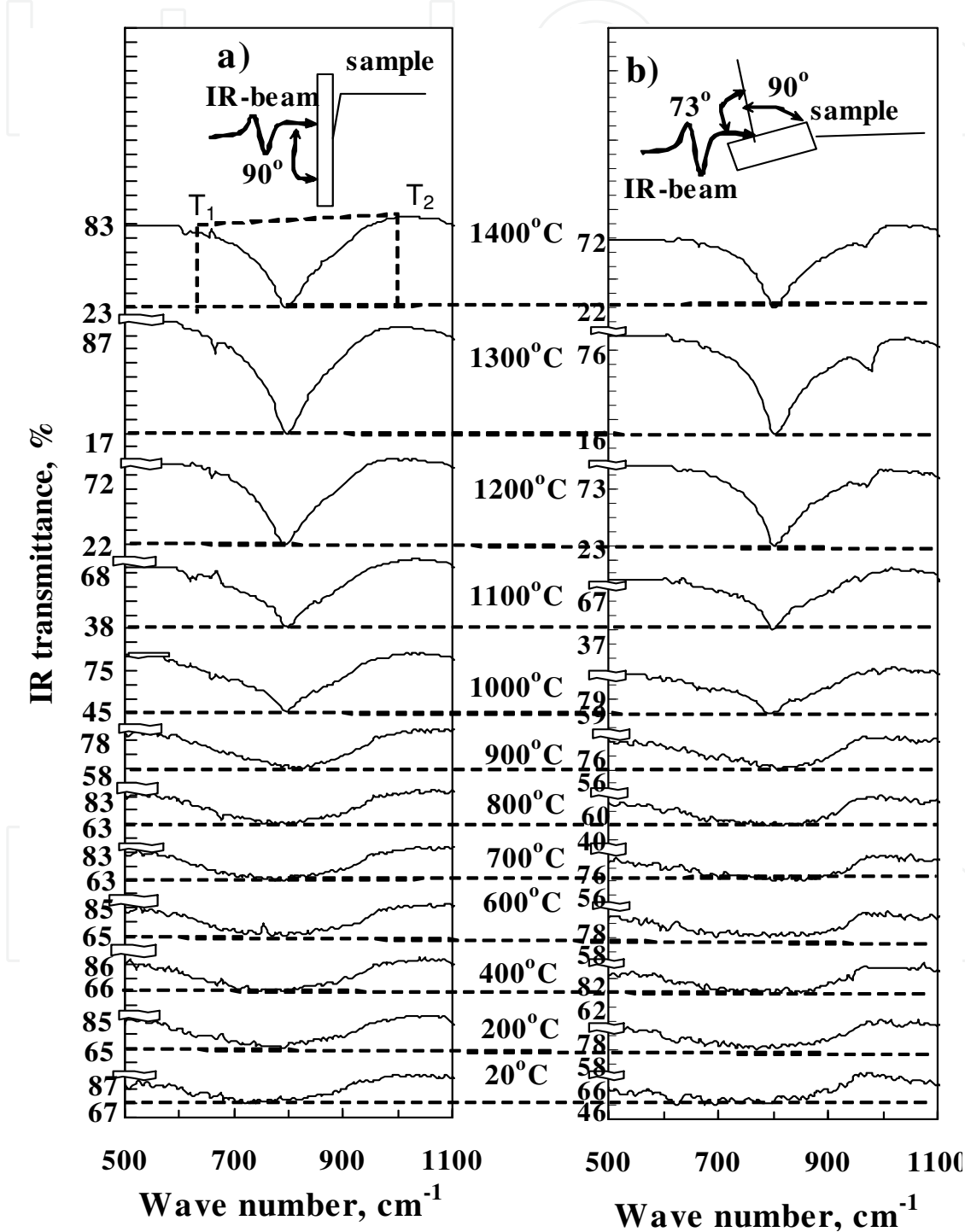

Fig. 16. IR transmission spectra of the SiC$_{1.4}$ layer recorded (a) under normal incidence of IR radiation on the sample and (b) at an angle of 73° to the normal to the sample surface.

At respecting certain condition, one can observe not only the transverse optical oscillations of atoms (TO-phonons), as well as longitudinal optical lattice oscillations (LO-phonons). For this purpose, we measured IR transmittance spectra of the implanted layers both at normal incidence of radiation on the sample, and at 73° to the normal to the surface (Figs. 16−21a, b). For a visual comparison of spectra from the SiC_x layers in Fig. 22 series of spectra of these layers before and after annealing at 600, 1000 and 1300°C measured at normal incidence of radiation on the sample, are presented. It is seen that among these layers a SiC-peak of the IR transmittance for the $SiC_{0.7}$ layer has maximum value of amplitude and minimum half-width after annealing at 1300°C. This implies a maximum number of tetrahedral oriented Si–C-bonds and high crystallinity of this layer, although the carbon concentration below the stoichiometric SiC. This phenomenon requires an explanation. For this purpose, an analysis of dependence of SiC-peak parameters on both annealing temperature and concentration of carbon for SiC_x layers was carried out.

It is well known that the spectral range 500−1100 cm^{-1} considered here includes the absorption bands corresponding to valence oscillations (in which the lengths of bonds vary predominantly) of the Si−C, C−C, and C−O-bonds, as well as deformation vibrations (in which the angles between the bonds are changed). As a result of interactions of these oscillations, it is impossible in principle to attribute the absorption band to individual bonds. If we assume that in the ideal case each type of Si−C-bonds corresponds to absorption at a certain frequency or in a narrow frequency interval, it can be concluded from the spectra in Figs. 16−22 that after implantation of carbon into silicon, the contour curve of the IR spectrum covers a large frequency (or wavenumber) range; i.e., the ion implanted layer contains a large number of different types of Si−C-bonds absorbing at different frequencies. Tetrahedral oriented Si−C-bonds with a length of 0.194 nm in crystalline silicon carbide absorb at the frequency corresponding to a wavenumber of 800 cm^{-1}, while the silicon layer amorphized by implantation of carbon ions contains Si−C-bonds with a length larger and smaller than this value and absorb at the frequencies slightly different from 800 cm^{-1}. This may be due to the fact that the stopping particles form a new Si−C-bonds which are not covalent because of variations in their length and in the angles between them. In the implanted amorphous Si−C-layer, one can also expect the presence of shorter double Si=C and triple Si≡C bonds, whose length is much smaller. Among the bonds can be present also the bonds, distances and angles between them (between atoms) are exactly the same as in the crystallite of SiC. For example, Kimura et al. (1981) by electron diffraction observed the crystallites of SiC immediately after implantation. In this case, one can observe non-zero absorption at a frequency of 800 cm^{-1} after implantation.

In addition, in the implanted layer can be expected the presence of long single bonds, free (dangling) bonds and hybridized Si−C-bonds, resonance and other higher order interactions. If the absorption of double C=C-bonds (1620-1680 cm^{-1}) and the triple C≡C-bonds (2100−2200 cm^{-1}) is beyond the study of the contour curve of the IR spectrum 500−1100 cm^{-1}, but the vibrations of C−C are in the region 900−1100 cm^{-1}. Nevertheless, the contribution to change the contour of the curve in this range and, in particular, to change the peak area will have a decay of single C−C, double C=C, Si=C or Si=Si, and triple C≡C, Si≡C or Si≡Si bonds, because of the formation after their decay of Si−C-bonds absorbing in this range (Silverstein et al., 1977].
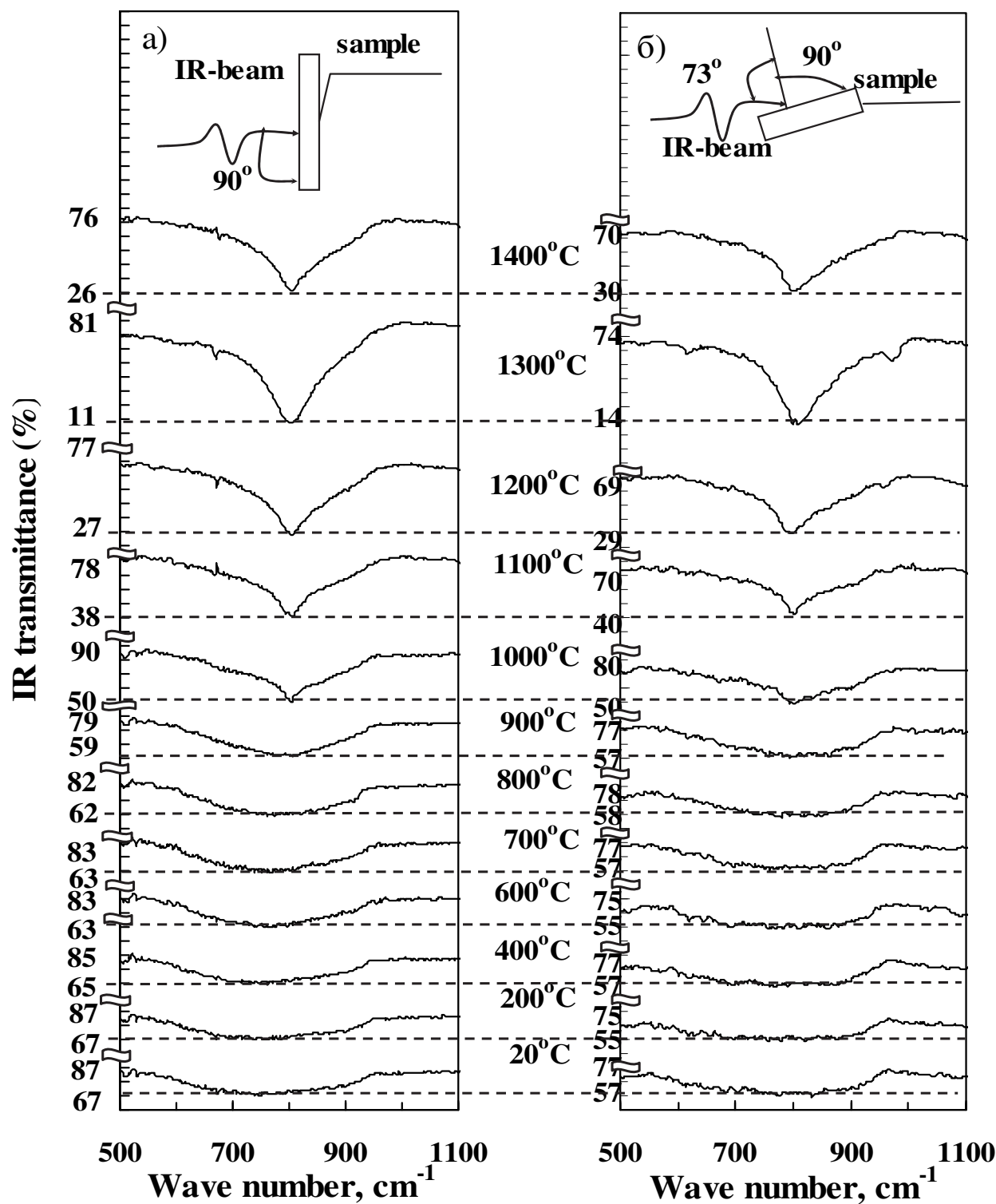
Fig. 17. IR transmission spectra of the SiC$_{0.95}$ layer recorded (a) under normal incidence of IR radiation on the sample and (b) at an angle of 73° to the normal to the sample surface.

Fig. 18. IR transmission spectra of the SiC$_{0.7}$ layer recorded (a) under normal incidence of IR radiation on the sample and (b) at an angle of 73° to the normal to the sample surface.
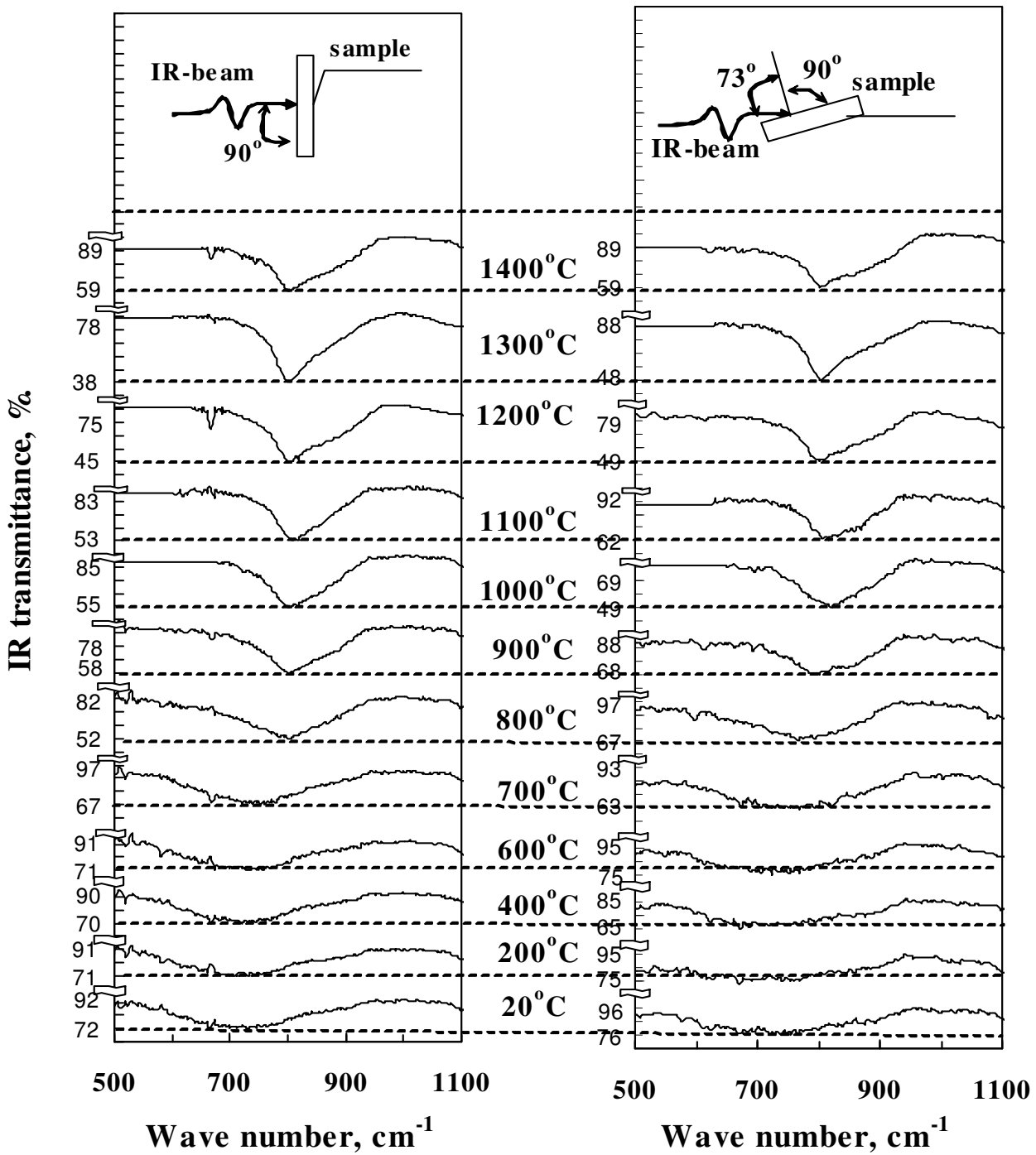
Fig. 19. IR transmission spectra of the SiC$_{0.4}$ layer recorded (a) under normal incidence of IR radiation on the sample and (b) at an angle of 73° to the normal to the sample surface.

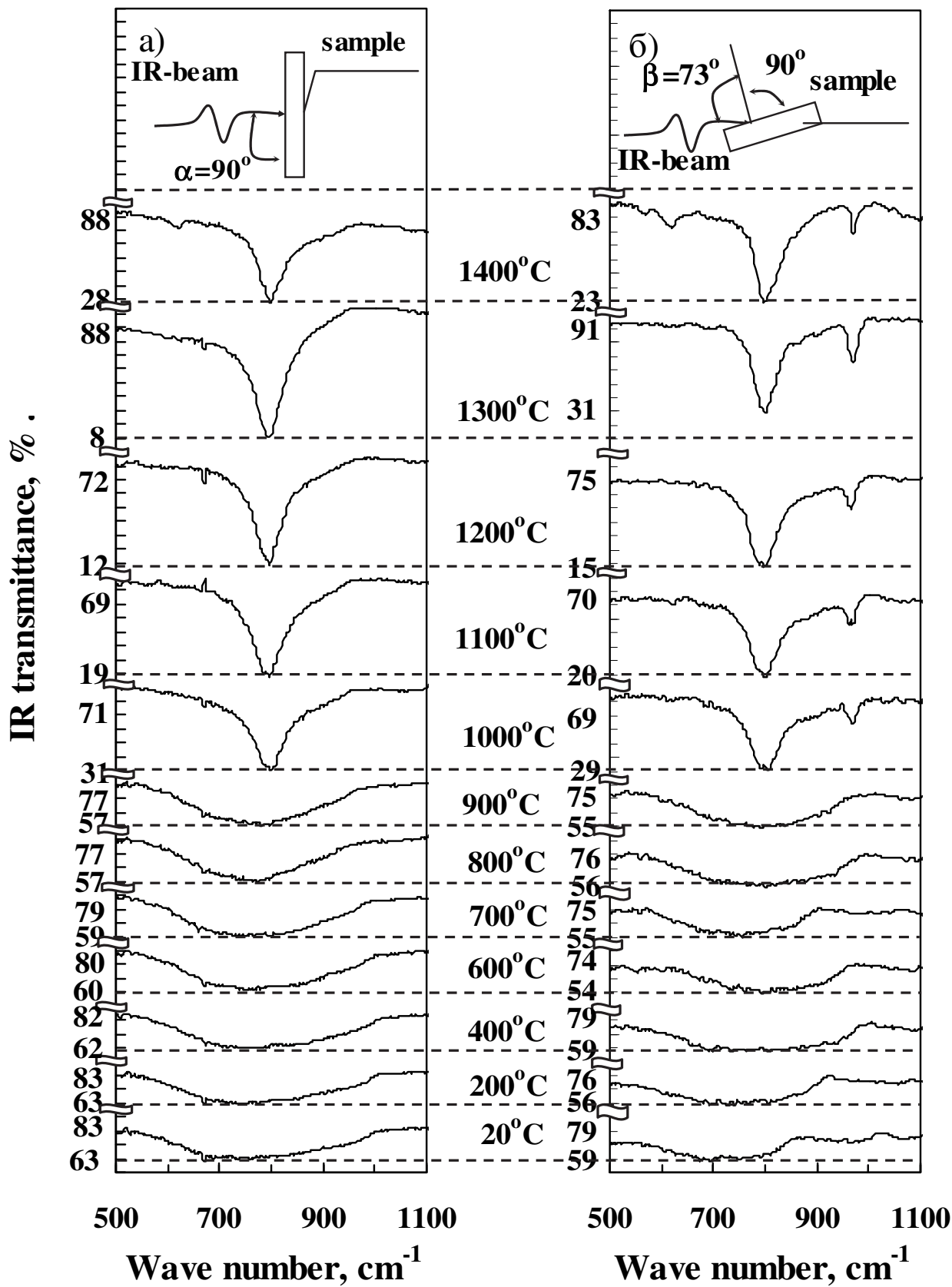Fig. 20. IR transmission spectra of the $SiC_{0.12}$ layer recorded (a) under normal incidence of IR radiation on the sample and (b) at an angle of 73° to the normal to the sample surface.
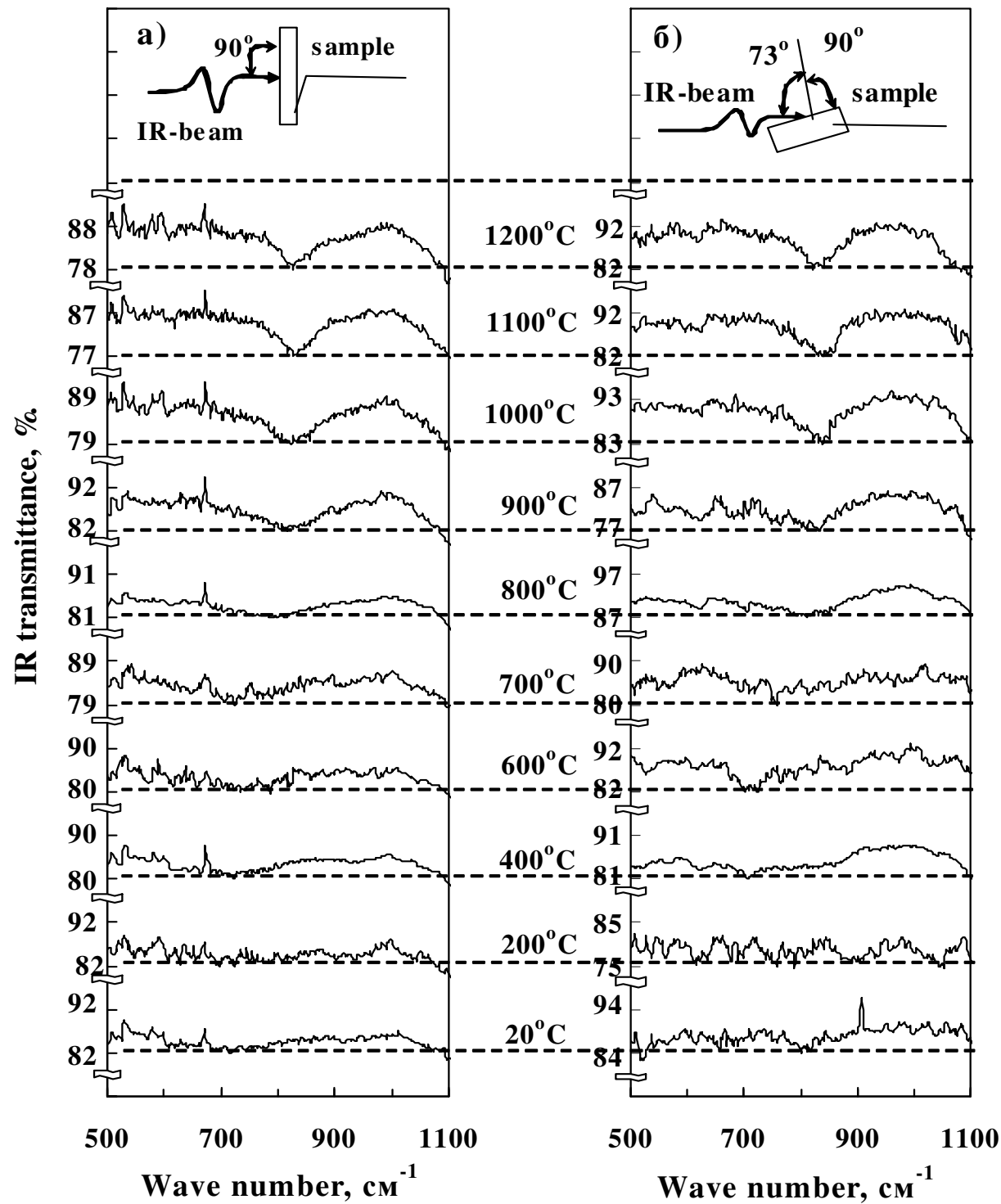
Fig. 21. IR transmission spectra of the SiC$_{0.03}$ layer recorded (a) under normal incidence of IR radiation on the sample and (b) at an angle of 73° to the normal to the sample surface.
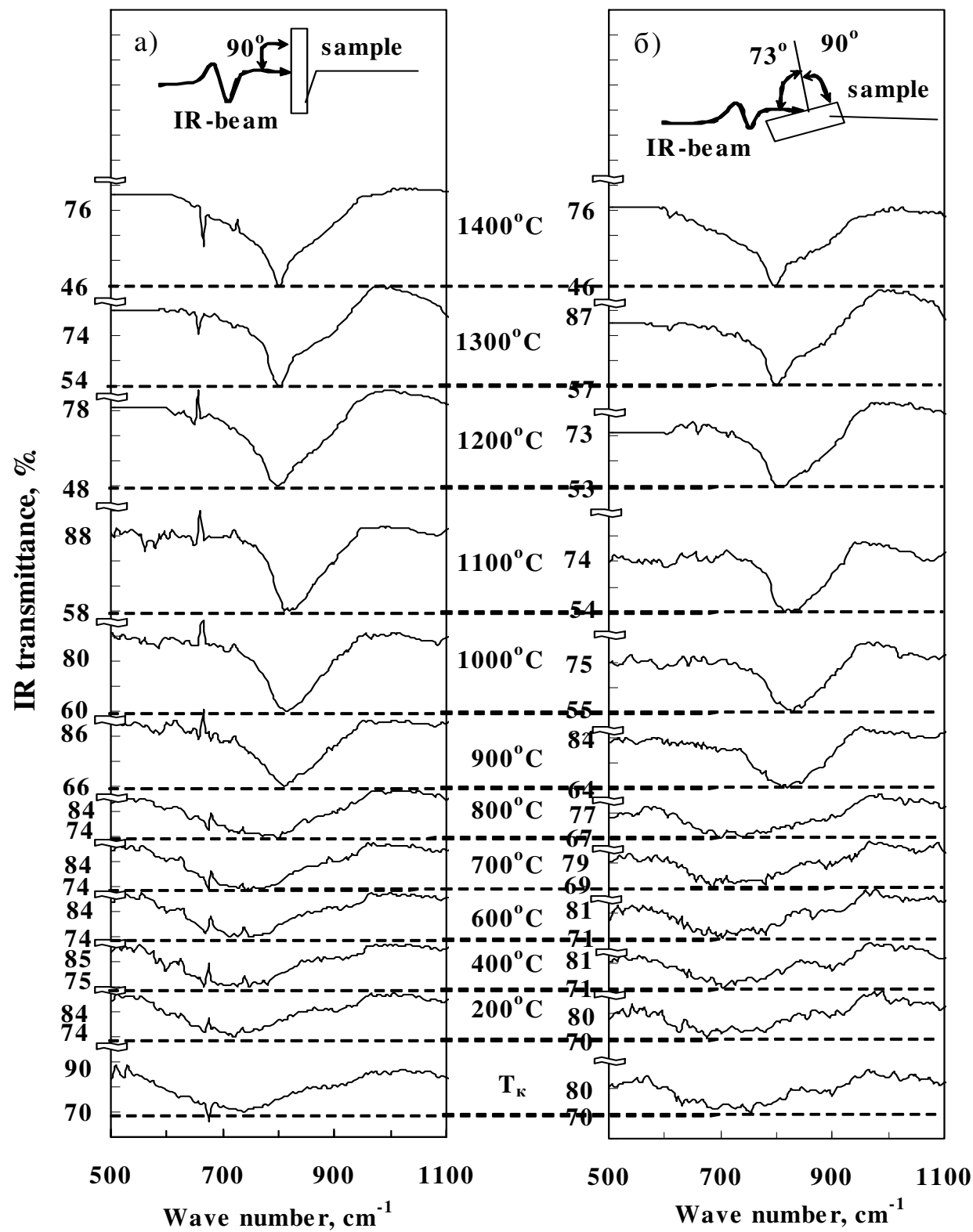
The position of the minimum of the IR transmission peak determines a certain type of bonds, which corresponds to the maximum of absorption at a given temperature. All layers considered here, exhibit after implantation, a transmission peak with the minimum at a frequency of 720−750 cm^{-1}, which is usually typical of amorphous silicon

carbide (Figs. 16-22). For the layers with low carbon concentration $SiC_{0.4}$, $SiC_{0.12}$ and $SiC_{0.03}$, the minimum of IR transmission is shifted in the region $720-725$ cm^{-1} to the left relative position of the minimum peak for the layers with a high concentration of carbon $SiC_{1.4}$, $SiC_{0.95}$ and $SiC_{0.7}$, located in the region $735-750$ cm^{-1} (Fig. 23). This may be due to the prevalence of long weak Si−C-bonds in the layers with low carbon concentration.
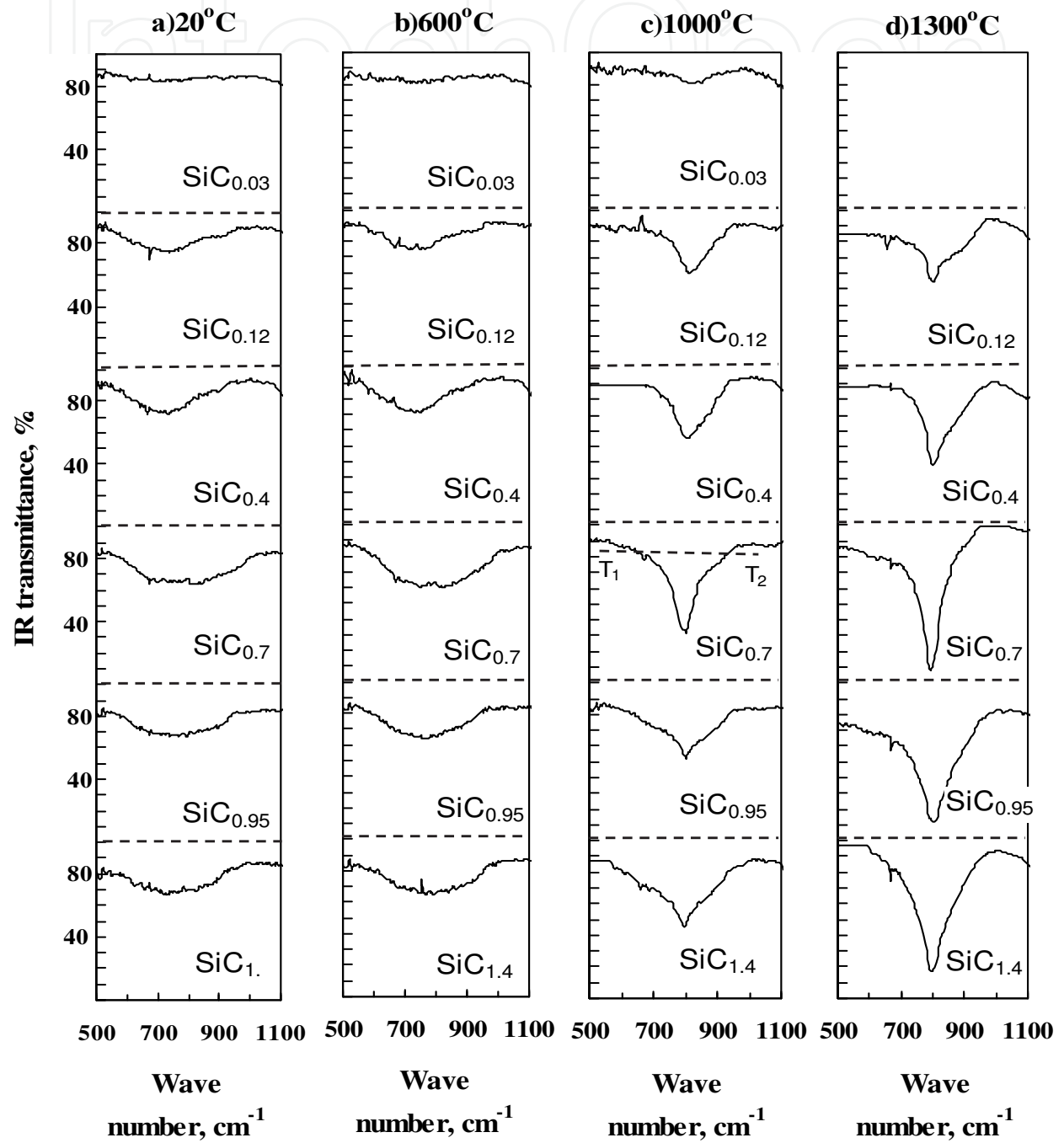

Fig. 22. IR transmission spectra of the $SiC_{1.4}$, $SiC_{0.95}$, $SiC_{0.7}$, $SiC_{0.4}$, $SiC_{0.12}$ and $SiC_{0.03}$ layers recorded after implantation of C^{12} ions (E = 40, 20, 10, 5 and 3 kev) into Si (a) and annealing for 30 min at temperatures 600°C (b), 1000°C (c) and 1300°C (d).

As a result of subsequent annealing, the peak is displaced to the right up to 800 cm⁻¹ (Fig. 23), indicating the formation of tetrahedral bonds typical of SiC, increases in amplitude and narrows. In the case of incidence of infrared radiation on the sample surface at the Brewster angle (73° from the normal), after annealing at 1000°C the appearance of the LO-phonon peak of SiC at frequency 955−965 cm⁻¹ is observed for the layers with a high concentration of carbon $SiC_{1.4}$, $SiC_{0.95}$ and $SiC_{0.7}$. With increasing of annealing temperature, this peak increases in amplitude synchronously with the peak of TO-phonons of silicon carbide (Figs. 16−18, 23). For layers with low carbon concentration $SiC_{0.4}$, $SiC_{0.12}$ and $SiC_{0.03}$ the LO-phonon peak of SiC was not observed (Fig. 19−21), which may be associated with small crystallite sizes of silicon carbide. At normal incidence of infrared radiation LO-phonon peak was not observed at both high and low concentrations of carbon (Figs. 16−21). Increase of the annealing temperature in the range 1000−1300°C results in some increase in the wavelength of the amplitude maximum of LO-phonon peak in the case of an excess of carbon for $SiC_{1.4}$ (Fig. 23, curve 1).

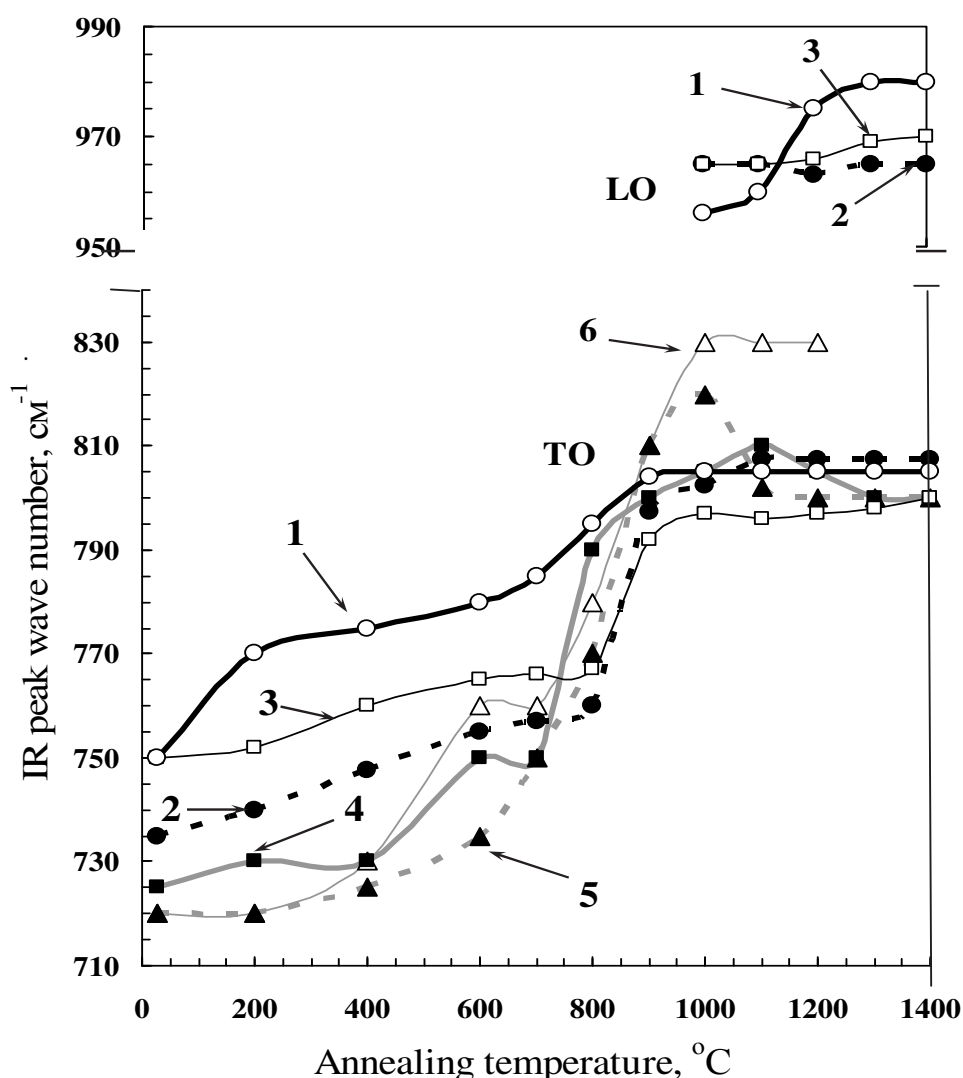Fig. 23. Wavenumber of the IR transmittance peak for TO- and LO-phonons SiC as a function of the annealing temperature: 1 - $SiC_{1.4}$, 2 - $SiC_{0.95}$, 3 - $SiC_{0.7}$, 4 - $SiC_{0.4}$, 5 - $SiC_{0.12}$, 6 - $SiC_{0.03}$.

In the case of layers with high concentrations of carbon, position of the minimum of IR transmission peak for TO-phonons is smoothly shifted from 750 to 805 cm^{-1} for $SiC_{1.4}$ with the increase of the annealing temperature in the range of 20−1000°C, from 735 to 807 cm^{-1} for $SiC_{0.95}$, from 750 to 800 cm^{-1} for $SiC_{0.7}$, indicating the formation of tetrahedral oriented Si−C-bonds characteristic of SiC (Fig. 23). The minimum of peak most intensively shifts after annealing in the range 800−900°C, which indicates on intensive processes of the layer ordering. Further annealing up to 1400°C does not lead to a noticeable shift of the minimum peak.

In several studies any changes in the IR transmission spectra have also not revealed after annealing at 1000°C (Borders et al., 1971) and 1100°C (Akimchenko et al., 1977b). This was attributed to the completion of the formation of β-SiC. However, as shown in Fig. 23 for $SiC_{1.4}$, $SiC_{0.95}$ and $SiC_{0.7}$ layers, if the curves of the peak position for TO phonons saturates and does not provide additional information in the temperature range 900−1400°C, then the curves for LO-phonon peak position undergo changes at these temperatures, indicating a structural change in ion-implanted layer. It can be assumed that the formation of tetrahedral Si−C-bonds of required length and angle between them is not completed up to 1300°C.

Although the shift of the minimum of the peak to 800 cm^{-1} indicating that tetrahedral Si−C-bonds prevail is observed at 1000°C, X-ray diffraction data show that the formation of SiC crystallites begins at 1000°C for $SiC_{0.7}$, 1150°C for $SiC_{0.95}$ and 1200°C for $SiC_{1.4}$ (Figs. 7 and 8), which means that Si−C-bonds are transformed into tetrahedral oriented bonds in the bulk of crystallites only at these temperatures. The increase in the intensity and number of X-ray lines of SiC upon an increase in the annealing temperature (Fig. 8) indicates an increase in the amount of SiC at the expense of the amorphous phase and perfection of its structure due to annealing of structural defects, respectively. It follows that the location of the minimum of transmission peak at ~800 cm^{-1} and the predominance of the tetrahedral oriented Si-C-bonds among the optically active bonds at temperatures 900−1000°C is not a sufficient condition for the formation of crystallites of silicon carbide in layers with high carbon content $SiC_{0.7}$ − $SiC_{1.4}$. At this temperature, a significant part of C and Si atoms can be incorporated in composition of an optically inactive stable clusters, which does not contribute to the amplitude of the IR transmission peak and are decompose at higher temperatures (>1150°C). This results an increase in the amplitude of the infrared transmission at a frequency of 800 cm^{-1} (Figs. 16, 18 and 22) at these temperatures.

Fig. 24 schematically shows the optically inactive Si−C-clusters, the atoms of which are connected by single, double and triple bonds, lie in one plane. In a flat optically inactive net the free (dangling) bonds to the silicon atoms (atoms №30 and 24) and carbon atoms (№21 and 27) are shown. Free bonds of these and other atoms (№ 4, 11, 12, 15, 17) can connected them with groups of atoms which do not lie on one plane and can form the association of optically active clusters. Since the distance between atoms № 22−4 and №5−22 are equal, the bond can oscillate forming 22−4 and 22−5. One double bond connected three atoms № 5, 6 and 7, i.e. there is the presence of resonance. The presence of two free bonds of the atom № 26 might lead to hybridization, i.e., association. Long single bonds between atoms № 2−3 and 1−18, which decay during low temperature annealing, are shown. Long optically inactive chains, and closed stable clusters of several atoms, connected to each other by double bonds, are also shown in Fig. 24.
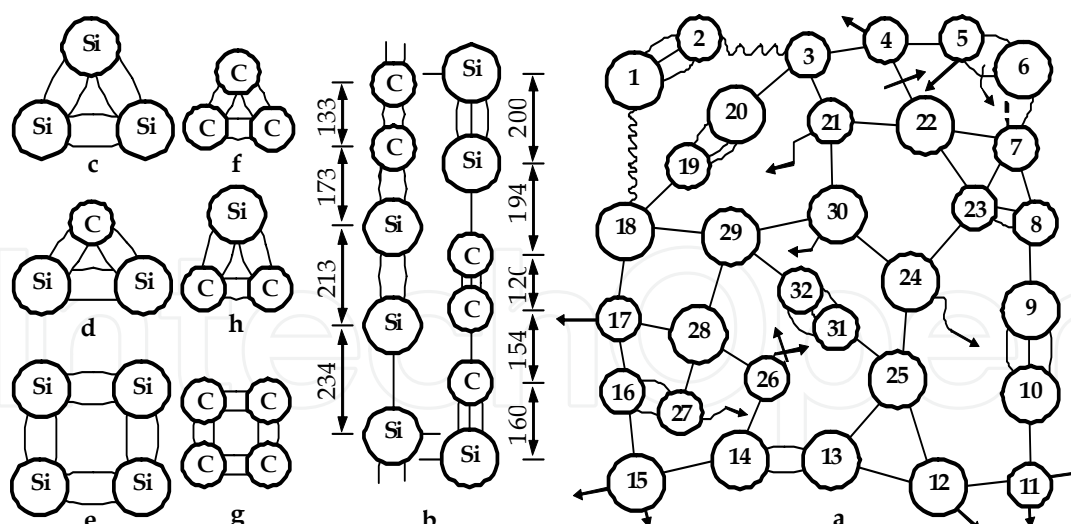
Fig. 24. Possible variants of both the infrared inactive clusters (a-h), chains of them (b) and a flat net of clusters (a) with various types of bonds between the atoms of Si (great circles) and C (small circles). Bond lengths are presented in pm.

It was found that for the layers SiC$_x$ with low carbon concentrations (Fig. 23), the minimum of IR transmission peak for the TO-phonons is shifted to above 800 cm^{-1} as the annealing temperature is increased. In the case of SiC$_{0.4}$ the position of the peak minimum shifts from 725 to 810 cm^{-1} in the temperature range 20−1100°C and returns to the 800 cm^{-1} at 1300°C. In the case of SiC$_{0.12}$ − from 720 to 820 cm^{-1} in the range 20−1000°C and returns to 800 cm^{-1} at 1200°C. In the case of SiC$_{0.03}$ – from 720 to 830 cm^{-1} in the range 20−1000°C and does not change its position during 1100−1200°C. Displacement of the peak minimum into the region above 800 cm^{-1} may be due to the presence of SiC nanocrystals of small size ($\leq$ 3 nm), and an increase in the contribution to the IR absorption amplitude of their surfaces and surfaces of the crystallites Si, containing strong shortened Si−C-bonds. For a layer SiC$_{0.12}$ and SiC$_{0.4}$, return of the minimum to 800 cm^{-1} at temperatures of 1100−1400°C may be caused by incorporation of carbon atoms into the nanocrystals of SiC and the growth of their size up to 3.5-5 nm and higher.

The observed shift of the peak minimum indicates the following fact: the absorbing at low frequencies energetically unfavorable long single Si−C-bonds decay during annealing at 600−1000°C, and the stronger short or tetrahedral Si−C-bonds absorbing at higher frequencies, are formed. Since the amplitude of IR transmission at 800 cm^{-1} is proportional to the concentration of tetrahedral oriented Si−C-bonds, and the amplitude at a certain frequency is assumed to be proportional to the absorption of Si−C-bonds at this frequency, we measured the IR transmittance amplitude for transverse optical (TO) phonons at wavenumbers of 700, 750, 800, 850 and 900 cm^{-1} after implantation and annealing at 200–1400°C (Fig. 25).

It can be seen from Figs. 25a–c that in the temperature range 20−1300°C, the amplitude of the peak at 800 cm^{-1} increases from 15 to 62% for the SiC$_{1.4}$ layer, from 14 to 68% for the SiC$_{0.95}$ layer, and from 18 to 87% for the SiC$_{0.7}$ layer. In the interval 20−900°C, the amplitude varies insignificantly. The maximal number of tetrahedral Si−C-bonds at 1300°C is observed in the SiC$_{0.7}$ layer. For these layers with high carbon concentration, the amplitudes of almost all frequencies (except 900 cm^{-1}) increase at 400°C, which can be due to ordering of the layer

and the formation of optically active Si−C-bonds. A certain increase in the amplitude at 800 cm^{-1} indicates the formation of tetrahedral Si−C-bonds at low temperatures.
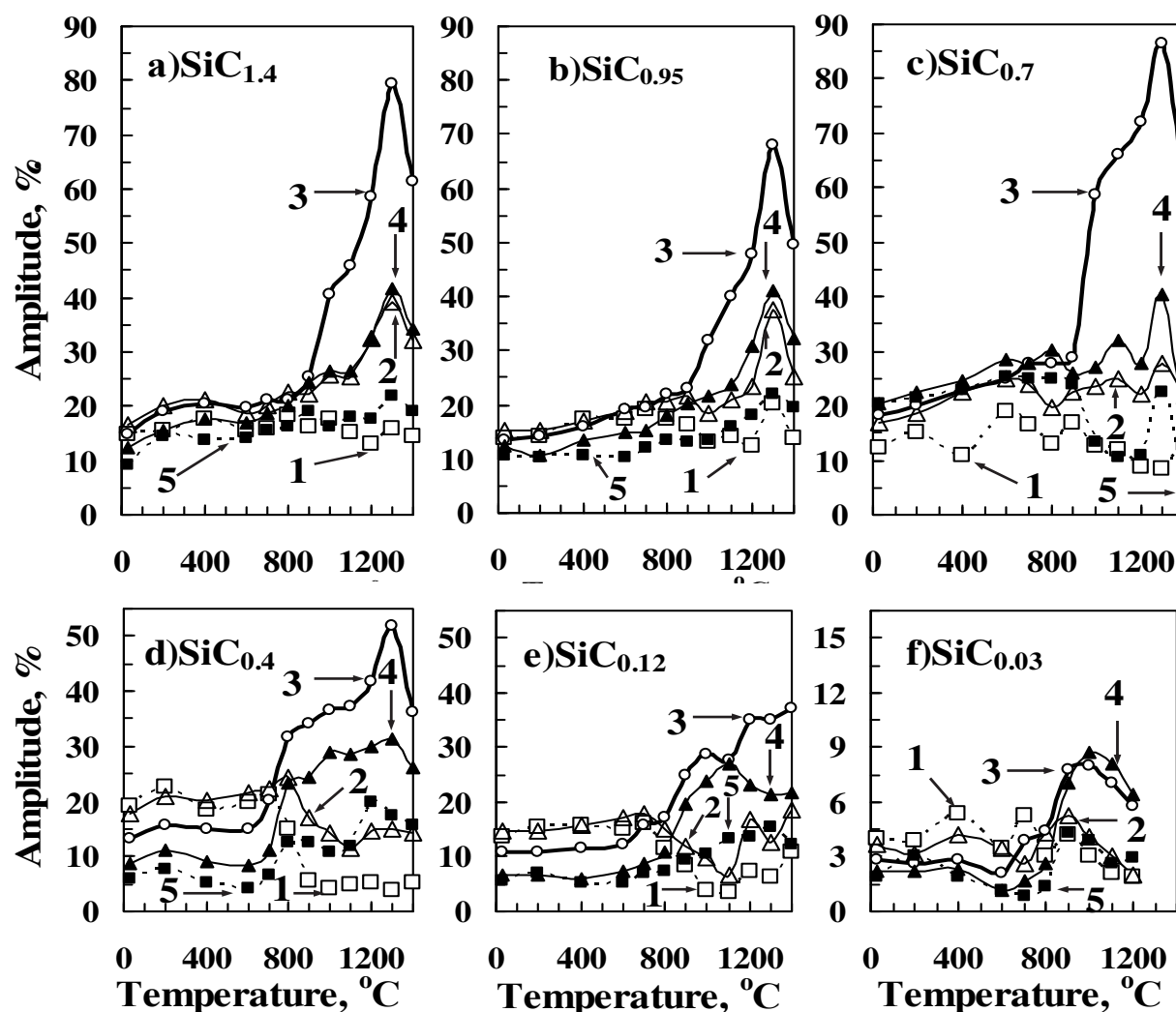

Fig. 25. Effect of the annealing temperature on the IR transmittance amplitude at wavenumbers of (1-□) 700 cm^{-1}, (2-Δ) 750 cm^{-1}, (3-○) 800 cm^{-1}, (4-▲) 850 cm^{-1}, and (5-■) 900 cm^{-1} under normal incidence of IR radiation on the sample surface: a) SiC$_{1.4}$; b) SiC$_{0.95}$; c) SiC$_{0.7}$, d) SiC$_{0.4}$, e) SiC$_{0.12}$; f) SiC$_{0.03}$.

The amplitudes at 800 cm^{-1} and close frequencies of 750 and 850 cm^{-1} considerably increase after annealing at temperatures in the interval 900−1300°C. This means that in SiC$_{1.4}$, SiC$_{0.95}$ and SiC$_{0.7}$ layers with a high carbon concentration, intense formation of tetrahedral Si–C bonds begins at 900−1000°C and continues up to 1300°C. This can be due to breakdown of carbon and silicon clusters (chains and flat nets) as well as single Si−C-bonds during annealing. The most pronounced decay of long single Si−C-bonds absorbing at a frequency of 700 cm^{-1} (Fig. 25a-c, curve 1) occurs during annealing at 800−1200°C. Annealing of SiC$_{1.4}$, SiC$_{0.95}$ and SiC$_{0.7}$ layers at 1400°C resulted in a decrease in the amplitudes in the entire frequency range 700−900 cm^{-1}, which is apparently due to decomposition of SiC as a result of carbon desorption from the layer. It can be seen from Fig. 25 that the dependences of IR transmission amplitudes on the annealing temperature for different wavenumbers for SiC$_{1.4}$, SiC$_{0.95}$ and SiC$_{0.7}$ layers with a

high carbon concentration are almost analogous, but differ considerably from the dependences for SiC$_{0.4}$, SiC$_{0.12}$ and SiC$_{0.03}$ layers with a low carbon concentration. This indicates the same nature of carbon and carbon–silicon clusters in SiC$_{1.4}$, SiC$_{0.95}$ and SiC$_{0.7}$ layers.

For SiC$_{0.4}$, SiC$_{0.12}$ and SiC$_{0.03}$ layers with a low carbon concentration, measurements of the IR transmission amplitude show (Figure 25, d-f) that in the temperature range 20–1300°C, the amplitude at 800 cm^{-1} increases from 13 to 52% for the SiC$_{0.4}$ layer, from 11 to 37% for the SiC$_{0.12}$ layer, and from 2.8 to 8% for the SiC$_{0.03}$ layer. At temperatures 20–600°C, in these layers dominate the long and weak Si−C-bonds, which absorb at frequencies of 700 and 750 cm^{-1} (Fig. 25d-f, curves 1 and 2) and decay at low temperatures. A noticeable increase in the amplitudes is observed at frequencies of 800 and 850 cm^{-1} in the temperature range 700−1000°C, which indicates an increase in the number of tetrahedral and nearly to tetrahedral short Si−C-bonds. A distinguishing feature for SiC$_{0.4}$, SiC$_{0.12}$ and SiC$_{0.03}$ layers with a low carbon concentration is an intense increase in the number of tetrahedral bonds at low temperatures (700°C), which is due to a low concentration of stable carbon clusters (chains, flat nets, etc.) disintegrating at higher temperatures, because low content of carbon atoms. Consequently, in the range of 800−900°C by the number of tetrahedral Si−C-bonds and the amplitude at 800 cm^{-1} (35%) the SiC$_{0.4}$ layers exceed all the above considered layers SiC$_{1.4}$, SiC$_{0.95}$, SiC$_{0.7}$. SiC$_{0.12}$ and SiC$_{0.03}$.

For SiC$_{0.4}$ and SiC$_{0.12}$ layers in the temperature range 700−1100°C, the increase in the amplitudes at frequencies of 800, 850, and 900 cm^{-1} is accompanied by a decrease in the amplitudes at 700 and 750 cm^{-1}, indicating an increase in the number of tetrahedral and strong short Si−C-bonds due to disintegration of long weak bonds that prevailed after implantation. Intensive formation of Si−C-bonds with the tetrahedral orientation, which absorb at a frequency of 800 cm^{-1} (Fig 25d and e, curves 3) at 1200°C is due to disintegration of strong optically inactive clusters of C and Si atoms. The SiC$_{0.4}$ layer with a higher carbon concentration differs from the SiC$_{0.12}$ layer because it contains stronger clusters disintegrating at 1300°C, which is manifested in a sharp increase in the amplitude at this temperature. As in the case of SiC$_{1.4}$, SiC$_{0.95}$ and SiC$_{0.7}$ layers with a high carbon concentration, the decrease in the amplitudes for SiC$_{0.4}$ at 1400°C is due to disintegration of SiC crystallites and desorption of carbon from the layer (Fig. 25d, curves 2–5).

Increase in the number of tetrahedral bonds in the layer SiC$_{0.03}$ in the temperature range 800−900°C occurs simultaneously with some increase in amplitude for all frequencies, i.e. not due to the decay of optically active bonds. For this layer with very low carbon concentration is difficult to assume the presence of a noticeable amount of stable carbon and carbon-silicon clusters. We can assume that a significant increase of tetrahedral bonds can occur by reducing the number of dangling bonds of carbon atoms.

We assume that the total area of the SiC-peak of IR transmission is the area of region between the curve of the IR spectrum and the baseline $|T_1T_2|$ (Fig. 16a), and it is equal to the total absorption of infrared radiation at all frequencies and is roughly proportional to the number of all types of absorbing Si−C-bonds (Wong et al., 1998; Chen et al., 1999). Peak area was determined from the spectra of IR transmission (Figs. 16−21), based on the approximation:

$$A = \frac{1}{2}(T_1 + T_2)(v_2 - v_1) - \int \tau(v)dv \approx \frac{1}{2}(T_1 + T_2)(v_2 - v_1) - \sum \tau(v)\delta v \,, \tag{2}$$

where A − total absorption (or transmission) in relative units in the frequency range $v_1<v<v_2$, $\tau(v)$ − transmission at frequency v, T_1 and T_2 − the values of IR transmission at frequencies v_1 and v_2, respectively, δv − step of measurements, equal to 2.5 or 5 cm^{-1}.

Fig. 26 shows the peak area of IR transmission for TO phonons as a function of the annealing temperature and the concentration of carbon for layers SiC$_{1.4}$, SiC$_{0.95}$, SiC$_{0.7}$, SiC$_{0.4}$, SiC$_{0.12}$ and SiC$_{0.03}$. It is seen that in the range of 27−1200°C the number of optically active Si−C-bonds is highest in the layer SiC$_{0.7}$. A smaller number of Si−C-bonds in the SiC$_x$ layers if x<0.7 is caused by lower carbon content, and if x>0.7 − due to the high concentration of stable clusters, decomposing at higher temperatures. Therefore, at 1300°C number of optical active Si−C-bonds is the highest in layer SiC$_{1.4}$.
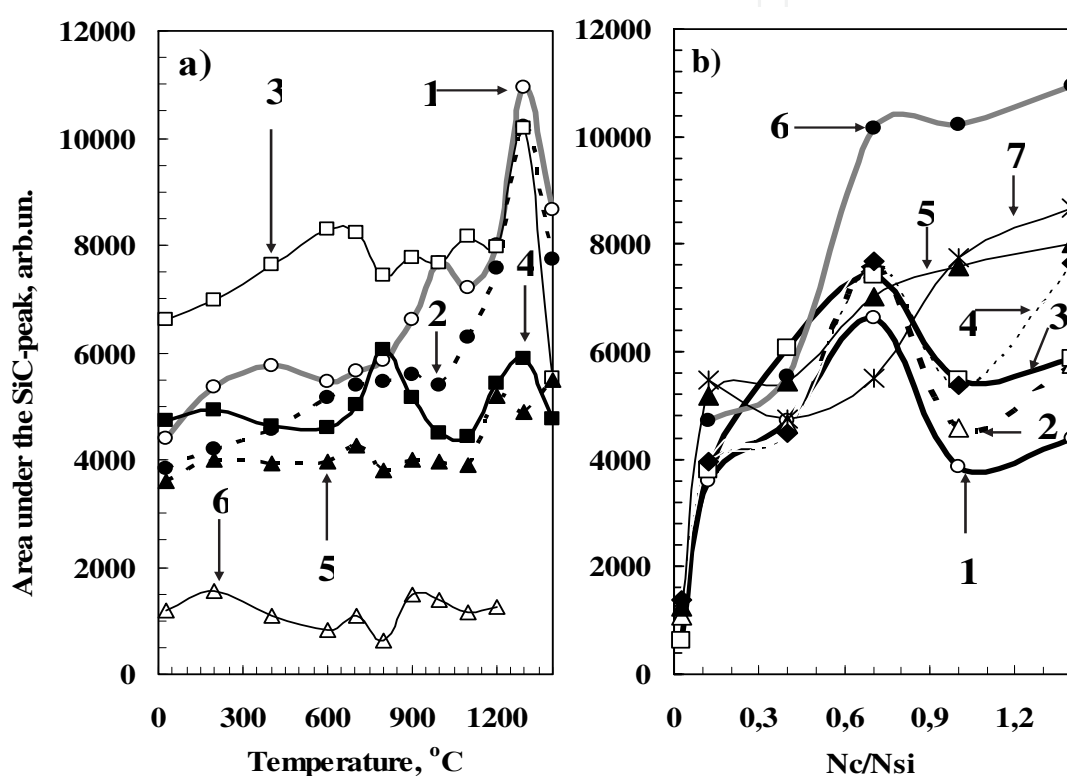

Fig. 26. Effect of the annealing temperature and concentration of carbon on the area under the IR transmittance SiC-peak for TO phonons under normal incidence of IR radiation on the sample surface: a) SiC$_{1.4}$ (1), SiC$_{0.95}$ (2), SiC$_{0.7}$ (3), SiC$_{0.4}$ (4), SiC$_{0.12}$ (5) и SiC$_{0.03}$ (6); b) 27 °C (1), 400°C (2), 800°C (3), 1000°C (4), 1200°C (5), 1300°C (6), 1400°C (7).

For layers SiC$_{1.4}$, SiC$_{0.95}$ and SiC$_{0.7}$ with high carbon concentration, the peak area of IR transmission immediately after implantation has the lowest value (Fig. 26a). In the temperature range 20−1400°C, the value of the peak area for SiC$_{1.4}$ is changed in the range of values within 4380–10950 arb. units, for SiC$_{0.95}$ − within 3850–10220 units, for SiC$_{0.7}$ − within 6620–10170 units, and tends to increase with annealing temperature, indicating a significant amount of carbon atoms do not bound with silicon in the layers immediately after implantation: ~[1−(4380/10950)×100/1.4] ≈ 70% for SiC$_{1.4}$, ~[1− (3850/10220)]×100% ≈ 62% for SiC$_{0.95}$, ~[1–(6620/10170)]×100% ≈ 35% for SiC$_{0.7}$. These estimates can be valid if we assuming that after annealing at 1300°C all clusters broke up and all carbon atoms formed optically active Si−C-bonds in the layer (except the excess atoms in SiC$_{1.4}$). In the case of a

partial decay of the clusters at 1300°C, the estimations of the proportion of carbon atoms included in the optically inactive clusters suggest even higher values. In general, the assertions do not contradict the data (Chen et al., 2003; Wong et al., 1998; Chen et al., 1999), where the growths of area of Si−C-peak after annealing, were shown. We evaluated the linearity of the dependence of the area and number of optically active Si−C-bonds on the carbon concentration, basing on data of the peak area (Table 4).

T, °C	A, arb. un.					
	SiC$_{0.03}$	SiC$_{0.12}$	SiC$_{0.4}$	SiC$_{0.7}$	SiC$_{0.95}$	SiC$_{1.4}$
20°C	1709	3588	4719	6622	3848	4384
200°C	1840	3990	4929	6966	4198	5347
400°C	1464	3921	4638	7647	4571	5757
600°C	1672	3979	4595	8296	5152	5442
700°C	1963	4248	5035	8227	5394	5665
800°C	1127	3795	6061	7428	5458	5864
900°C	1924	4004	5150	7772	5571	6619
1000°C	2708	3958	4499	7674	5386	7664
1100°C	2069	3910	4437	8158	6296	7190
1200°C	2428	5181	5428	7980	7570	8011
1300°C	0	4886	5805	10169	10221	10953
1400°C		5473	4749	5510	7741	8670

Table 4. Area, A, under the IR transmittance SiC-peak for TO phonons obtained from the IR spectra for SiC$_x$ layers after implantation and annealing

In the layer SiC$_{0.03}$ the number of optically active Si−C-bonds after annealing should be roughly proportional to the quantity of carbon atoms due to the low concentration of carbon and stable carbon or carbon-silicon clusters as well. We take the maximum value of the area of Si−C-peak for the SiC$_{0.03}$ layer at 1000°C as equal to 1. If the proportionality is linear, an increase in the concentration of carbon in SiC$_x$ layer on n_1 times ($n_1 = (N_C/N_{Si})/0.03 = x/0.03$) should increase the peak area on n_2 times ($n_2 = A_x(T)/A_{0.03}(1000°C)$), and $n_1 = n_2$, if not come saturation in the amplitude of the transmission, and the carbon atoms are not included in the optically inactive clusters. Since the saturation amplitude of the IR transmission is not reached (Fig. 25) and $n_2 < n_1$, so a values $100\% \times n_2/n_1$ show the portion of carbon atoms forming optically active Si−C-bonds in the SiC$_x$ layer. As it turned out, at 1300°C in the layer SiC$_{1.4}$ only 9% of the C atoms form the optically active Si−C-bonds, in SiC$_{0.95}$ − 12%, in SiC$_{0.7}$ and SiC$_{0.4}$ − 16%, in SiC$_{0.12}$ − 45%, while the other carbon atoms remain in the composition of strong clusters. The total number of SiC (optically active Si−C-bonds) in the SiC$_x$ layers after annealing at 1300°C increases with the fractional degree of carbon concentration $(x/0.03)^y$, where $y \sim 0.37 \pm 0.09$ (Table 5).

In (Wong et al., 1998) at a fixed energy the total number of formed SiC increases with the fractional degree of doses, namely, D^y witg «y» defined as 0.41. In this paper, SiC layers were synthesized using the ion source MEVVA implantation in p-Si of carbon ions with energies in the range 30−60 keV and doses ranged within $(0.3–1.6) \times 10^{18}$ см$^{-2}$. In this case, the infrared absorption spectra of SiC layers were decomposed into two or three components, one of which belonged to the amorphous SiC, while the other two to β-SiC.

Really, as seen in Table 5, the increase of carbon concentration x in the layer $SiC_{0,12}$ in 4 times in comparison with $SiC_{0.03}$ results to a smaller increase in the area of SiC-peak, pointing to the disproportionate increase in the number of optically active Si−C-bonds . At least, the maximum area at 1200°C for a $SiC_{0.12}$ layer exceeds the maximum area for $SiC_{0.03}$ layer only in 1.91 times. Further increase in the concentration of carbon x in the SiC_x layers in 13, 23, 32, 47 times leads to an increase in the number of optically active Si−C-bonds in several times less than expected − no more than 4.04 times even for high temperature annealing.

Both the peak areas and the number of bonds do not increase linearly with the increase of concentration and it is not caused by saturation of amplitude values. As in the case of N_C/N_{Si} = 0.12, the increase of concentration in 13.3 times at N_C/N_{Si} = 0.4, has led to an increase in the amplitude of only 9 times, and an area of 2.1 times (5805 un.) at 1300°C (Tables 4 and 5), although the amplitude of the IR transmittance at the minimum of the peak is far from saturation (52%). This confirms that the determining factor is the presence of strong clusters, in the structure of which is included the majority of the carbon atoms. That is at 1300°C in the $SiC_{0.4}$ layer only n_1/n_2 = 2.1/13.33 = 16% of the carbon atoms form an optically active Si−C-bonds, and in the $SiC_{0.12}$ layer − 45%. Then, in the optically inactive stable clusters are included the rest 84% and 55% of carbon atoms (Table 5), respectively, resulting in no increase in peak area proportionally to the concentration of carbon. Since there is a predominance of the tetrahedral oriented bonds among the optically active Si-C-bonds, the amount of tetrahedral Si−C-bonds is sufficient for the appearance of SiC crystallites in the layers, which is observed on the X-ray diffraction pattern.

SiC_x	$SiC_{0.03}$		$SiC_{0.12}$		$SiC_{0.4}$		$SiC_{0.7}$		$SiC_{0.95}$		$SiC_{1.4}$	
$n_1=x/0.03$	1.0		4.0		13.3		23.3		31.7		46.7	
T, °C	$\frac{A_x}{A_{0.03}}$	Si-C %	$\frac{A_x}{A_{0.03}}$	Si-C %	$\frac{A_x}{A_{0.03}}$	Si-C %	$\frac{A_x}{A_{0.03}}$	Si-C %	$\frac{A_x}{A_{0.03}}$	Si-C %	$\frac{A_x}{A_{0.03}}$	Si-C %
20	0.63	63	1.3	33	1.7	13	2.4	10	1.4	4	1.6	3
200	0.68	68	1.5	37	1.8	14	2.6	11	1.6	5	2.0	4
400	0.54	54	1,4	36	1.7	13	2.8	12	1.7	5	2.1	5
600	0.62	62	1.5	37	1.7	13	3.1	13	1.9	6	2.0	4
700	0.72	72	1.6	39	1.9	14	3.0	13	2.0	6	2.1	4
800	0.42	42	1.4	35	2.2	17	2.7	12	2.0	6	2.2	5
900	0.71	71	1.5	37	1.9	14	2.9	12	2.1	6	2.4	5
1000	1.00	100	1.5	37	1.7	12	2.8	12	2.0	6	2.8	6
1100	0.76	76	1.4	36	1.6	12	3.0	13	2.3	7	2.7	6
1200	0.90	90	1.9	48	2.0	15	2.9	13	2.8	9	3.0	6
1300		90	1.8	45	2.1	16	3.8	16	3.8	12	4.0	9
y(1300°C)			0.40		0.28		0.42		0.38		0.36	

Table 5. Relative values of area (n_2 = A_x(T)/$A_{0.03}$(1000°C)) of IR transmission SiC-peak and the proportion of carbon atoms (100% × n_2/n_1) which forms an optically active Si-C-bonds in the SiC_x layers.

Evaluation results may be debatable, since the literature contains different points of view concerning inclusion of carbon into SiC. Akimchenko et al. (1977a) after implantation of Si (E = 40 кэВ, D = 3.7×10^{17} см$^{-2}$) in diamond and annealing at temperatures of 500-1200°C assumed that almost 100% of implanted carbon atoms included in the SiC. This conclusion was made from accordance of calculated layer thickness (80 nm) with ones found from the absorption near 810 cm^{-1} (70 nm). A comparison with the magnitude of the SiC thickness (8−10 nm) obtained by X-ray diffraction, allowed to conclude that 10−15% of atoms of the disordered SiC united into β-SiC crystallites, which contribute to the X-ray reflection, and the rest remains in the amorphous state. Kimura et al. (1982) basing on data from the optical density of the infrared transmission spectra have established that all implanted carbon are included in β-SiC after annealing at 900−1200°C, if the concentration of implanted carbon is less or equal to the stoichiometric composition of SiC at the peak of the distribution. In the case of higher doses, the excess carbon atoms form clusters and are not included into β-SiC, even after annealing at 1200°C. The activation energy required for inclusion of carbon atoms in the β-SiC, increases with increasing of implantation doses, since more energy is required for the decomposition of carbon clusters. Durupt et al. (1980) showed that if the annealing temperature below 900°C, the formation of SiC is less pronounced in the case of high dose, and annealing at higher temperature removes the differences.

On the other hand, Borders et al. (1971) from the infrared absorption and Rutherford backscattering data found that about half of carbon atoms implanted into the silicon (E = 200 кэВ, D = ~10^{17} см$^{-2}$) included in micro-SiC. According to our estimates, the concentration of carbon atoms in the layer was lower than 10% (x <0.1). Kimura et al. (1981) from the analysis of infrared spectra revealed that after implantation (E = 100 keV) and annealing at 900°C about 40-50% of carbon atoms united with Si atoms to form β-SiC, and this value monotonically increased to 70-80% with increasing of annealing temperature up to 1200°C. The number of carbon atoms included in the β-SiC was affected by dose of carbon ions. Calcagno et al. (1996) showed that the optical band gap and the intensity of the infrared signal after annealing at 1000°C increased linearly with carbon concentration, reaching a maximum at the stoichiometric composition of SiC. At higher carbon concentrations intensity of the infrared signal undergoes saturation, and the band gap decreases from 2.2 to 1.8 eV. By Raman spectroscopy is shown that this is due to the formation of clusters of graphite. Simon et al. (1996) after the high-temperature (700°C) implantation of carbon ions into Si (E = 50 keV, D = 10^{18} and 2×10^{18} см$^{-2}$) show that the carbon excess precipitates out, forming carbon clusters. It is assumed that the stresses and defects, formed after the first stage of implantation, form traps, which attract the following carbon atoms. Liangdeng et al. (2008) after implantation of C ions (E = 80 keV, D = 2.7×10^{17} ион/см^{2}) in the Raman spectra observed double band with center in 1380 and 1590 cm^{-1} corresponding to the range of graphitized amorphous carbon. The authors suggest that since solid solubility of carbon in a-Si at a temperature close to the melting point of Si, is about 10^{17}/cm^{3}, and almost disappears at room temperature, the carbon has a tendency to form precipitates. Bayazitov et al. (2003) after implantation of carbon ions (E = 40 keV, D = 5×10^{17} см$^{-2}$) in silicon and pulsed ion beam annealing (W = 1.0 J/cm^{2}, C^{+}(~80%) and H^{+}(~20%)) have formed a β-SiC layer with an average size of grain about 100 nm. Increasing the energy density per pulse up to 1.5 J/cm^{2} leads also to appearance of graphite grains of sizes about 100 nm, as well as visually observed darkening of the sample. When exposed by radiation of ruby laser (λ = 0.69 μm, τ = 50 nsec, W = 0.5-2 J/cm^{2}) also formed the graphite grains, beginning from W = 0.5 J/cm^{2}.

Tetelbaum et al. (2009) by implantation in SiO_2 film of Si ions (E = 100 keV, D = 7×10^{16} cm^{-2}) provided the concentration of excess silicon at the peak of the ion distribution about 10 at.%. Then the same number of carbon atoms was implanted. The obtained data of the white photoluminescence with bands at ~400, ~500 and ~625 nm, attributed to nanoinclusion of phases of SiC, C, nanoclusters and small nanocrystals Si, respectively (the arguments supported by references to the results of Perez-Rodrıguez et al. (2003) and Fan et al. (2006)). Similarly, Zhao et al. (1998) received a peak at 350 nm, and a shifting by the annealing the blue peak at 410−440, 470, 490 nm. The existence of inclusions phases of carbon and silicon carbide in the films of SiO_2 in (Tetelbaum et al., 2009) was confirmed by X-ray photoelectron spectroscopy by the presence of the C−C (with energy ~285 eV) and Si−C (with energy ~283 eV). Comparing the amplitudes I_{RFS} one can conclude that a number of C−C is comparable to the number of Si−C-bonds, and a luminescence at 500 nm (carbon clusters) is considerably greater than the luminescence at 400 nm (silicon carbide). Belov et al. (2010) used higher doses of carbon ions (E = 40 keV): 6×10^{16} см$^{-2}$, 9×10^{16} см$^{-2}$ and 1.2×10^{17} см$^{-2}$, in which the concentration of carbon (by our estimation) do not exceed 25% at the maximum of the carbon distribution. The authors believe that the luminescent centers, illuminated at wavelengths below 700 nm, represent the nanoclusters and nanocrystals of (Si:C), and amorphous clusters of diamond-like and graphitized carbon. In this case, with increasing of carbon doses the intensity of photoluminescence from Si nanocrystals (>700 nm) varies little, and concluded that a significant portion of the implanting carbon is included into the carbon clusters. The high content of graphitized clusters in the films also discussed in (Shimizu-Iwayama et al., 1994). All these data suggest that a significant or most of the carbon atoms are composed of carbon clusters, although the concentration of carbon atoms in a layer of "SiO_2 + Si + C" was around 9 at.%. In our opinion, this confirms our high estimates of carbon content in the optically inactive C- and C−Si-clusters, made basing the analysis of IR spectra. Analysis of the behavior of the curves in Fig. 26 may be interesting from the point of studying the influence of decay of clusters and Si−C-bonds on the formation of tetrahedral oriented Si-C-bonds. Basing on the analysis one can suggest possible mechanisms of formation of silicon carbide grains in the layer and put forward a number of hypotheses. For example, the growth curves of SiC-peak area for the $SiC_{1.4}$, $SiC_{0.95}$ and $SiC_{0.7}$ layers with a high carbon concentration have the maxima of values, which may be related with the formation and breaking of bonds and clusters in the implanted layer. Intensive growth of area in the range 1100−1300°C caused by the decay of stable optically inactive clusters (Table 5) and an increase in the number of all types of Si−C-bonds absorbing at all frequencies of considered range, in particular, the tetrahedral oriented bonds (800 cm^{-1}). However, the growth of these bonds (curves 3 in Figure 25) is not always accompanied by an increase in area under the IR transmittance peak.

Variation of the peak area for the $SiC_{1.4}$ layer (Fig. 26) has peaks at 400, 1000 and 1300°C. The growth of the peak area in the range of 20−800°C for $SiC_{1.4}$, $SiC_{0.95}$ and $SiC_{0.7}$ layers with high carbon concentrations is caused by a weak ordering of the amorphous layer and the formation of optically active Si−C-bonds, including the tetrahedral oriented bonds (Fig. 25a). Significant growth of area in the range 800−1000°C is resulted by an increase of the absorption in the range 800±50 cm^{-1}, i.e. by an intensive formation of the tetrahedral and near tetrahedral Si−C-bonds due to the decay of such optically inactive clusters as flat nets and chains (Fig. 24). Decrease of Si−C-peak area (Fig. 26, curves 1 and 3) in ranges of 400−600°C or 600−800°C caused by decay of long single bonds absorbing near 700 or 750 cm-

[1] (Fig. 25a, curves 1 and 2). Decrease in area at 1400°C is associated with a decrease in amplitude at all considered frequencies, especially at 800 cm^{-1}, indicating that the decay of a large number of tetrahedral Si-C-bonds and desorption of ~ 15% of carbon atoms are taken place.

As shown in Fig. 26 (curve 3), the number of optically active **Si−C**-bonds in the temperature range 20−1200°C is the highest for the layer SiC$_{0.7}$. In the temperature range 20−1300°C, the amplitude at 800 cm^{-1} increases in 4.4 times from 20 to 87%, while the area of **SiC**-peak grow only in 3.76/2.45 = 1.54 times.. It follows that growth in the number of tetrahedral bonds is taken place not only due to the decay of optically inactive **Si−C**-clusters, but as a result of decay of long single **Si−C**-bonds as well, which absorb at a frequency of 700 cm^{-1} (Fig. 25c, curve 1), with their transformation into a tetrahedral (curve 3) and close to tetrahedral (curve 4) bonds, which absorb near 800 and 850 cm^{-1}. Most intensively this process occurs near the surface of SiC crystallites (Fig.12b) in the range 900−1300°C showing the mechanism of the formation of SiC crystallites.

The temperature dependence of both the amplitude of the IR transmission at different wave numbers and the area of SiC-peak for the SiC$_{1.4}$, SiC$_{0.95}$ and SiC$_{0.7}$ layers has a similar character, which, as it was mentioned above, indicates the common nature of carbon and carbon-silicon clusters in these layers with a high concentration of carbon. Analysis of the behavior of the curves in Fig. 26 (curves 4, 5 and 6) shows that the curves of the area changes of the peak for the SiC-layers with low carbon concentration SiC$_{0.4}$, SiC$_{0.12}$ and SiC$_{0.03}$ also have the maxima and minima of magnitude, which can be associated with the formation and breaking of bonds and clusters. These layers are characterized by an higher proportion (%) of carbon atoms forming an optically active Si−C-bonds (Table 5), although the total number is low in comparison with SiC$_{1.4}$, SiC$_{0.95}$ and SiC$_{0.7}$ layers (Fig. 26).

The value of the area for the SiC$_{0.4}$ layer in the temperature range 20−1400°C has not a continuous upward trend. Maximum of area at 800°C is due to the formation of tetrahedral and close to tetrahedral bonds, absorbing near 800 and 850 cm^{-1} (Fig. 25d, curves 3 and 4), respectively. The formation of tetrahedral bonds (800 cm^{-1}) at temperatures of 900−1100°C (Fig. 25d, curve 3) is accompanied by decreasing of peak area due to its narrowing resulting from the decay of long single **Si−C**-bonds, which absorbed near 700 and 750 cm^{-1} and prevailed at temperatures below 800°C. The formation of Si and SiC crystallites in the layer is taken place almost simultaneously, which suggests intense movement of C and Si atoms and the increase in the number of dangling bonds. The increase in area in the range 1200−1300°C (Fig. 26) is caused by growth of tetrahedral (Fig. 25, curve 3) and close to tetrahedral (Fig. 25, curves 2 and 4) **Si−C**-bonds due to decay of optically inactive clusters.

For layers SiC$_{0.12}$ and SiC$_{0.03}$ with carbon concentration much lower than stoichiometric for SiC, the absence of significant growth of area in the temperature range 200−1100°C is revealed due to the small amount of optically inactive unstable carbon flat nets and chains, the decay of which could cause an intensive formation of absorbing bonds. Nevertheless, a significant increase in amplitude at 800 cm^{-1} is observed due to the formation of tetrahedral bonds. Increase in the area after annealing at 900−1000°C for the SiC$_{0.03}$ layer together with growth of the amplitudes of all types of optically active **Si−C**-bonds may be caused by the formation of silicon crystallites, which accompanied by the displacement of carbon atoms and a reduction in the number of dangling bonds of carbon atoms. For layers SiC$_{0.12}$ and SiC$_{0.4}$ the significant growth of area at temperatures 1200−1300°C caused by an increase in the number of all types of optically active bonds due to decay of stable carbon clusters.

The half-width of the Si−C-peak of IR transmission were measured (Fig. 27). Narrowing of the peak occurs due to intensive formation of tetrahedral oriented Si−C-bonds, absorbing at 800 cm^{-1}, and decay of bonds, which absorb at frequencies far from the value of 800 cm^{-1}. Since the tetrahedral bonds correspond to the crystalline phase of silicon carbide, so the narrowing of the SiC-peak of the IR spectrum is related with the processes of the implanted layer ordering. For a layer SiC$_{1.4}$ a sharp narrowing of the peak from 300 to 110 cm^{-1} is taken place in the range 800−1200°C, and then the half-width does not change significantly. The most intensively this process occurs in the range 900−1000°C. On X-ray diffraction patterns (Fig. 7), the appearance of lines of polycrystalline β-SiC was observed after annealing at 1200°C and above. This implies that the appearance of SiC crystallites in the layer is recorded when the formation of tetrahedral bonds (peak narrowing) is substantially complete (110 cm^{-1}). Assumptions about the relationship between the size of SiC crystallites and half-width of the peak were also expressed in (Wong et al., 1998; Chen et al., 1999). For the SiC$_{0.7}$ layer in range 900−1000°C, a sharp narrowing of the peak from 280 to 85 cm^{-1} is taken place and occurred more intensive up to 67 cm^{-1} at 1200°C than for layers with a higher carbon concentration SiC$_{0.95}$ (115 cm^{-1}, 1200°C) and SiC$_{1.4}$ (108 cm^{-1}, 1300°C), indicating a much lower concentration of strong clusters in the layer SiC$_{0.7}$.
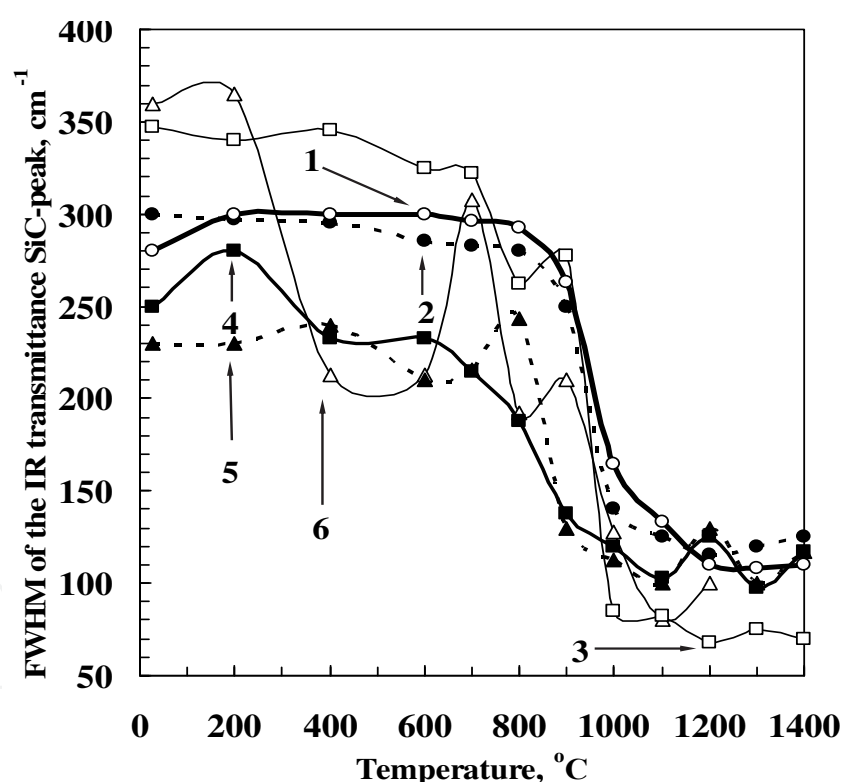

Fig. 27. Effect of the annealing temperature on the FWHM of the IR transmittance SiC-peak for TO phonons under normal incidence of IR radiation on the sample surface: 1 − SiC$_{1.4}$, 2 − SiC$_{0.95}$, 3 − SiC$_{0.7}$, 4 − SiC$_{0.4}$, 5 − SiC$_{0.12}$, 6 − SiC$_{0.03}$.

For a layer SiC$_{0.12}$, a sharp narrowing of the peak from 240 to 100 cm^{-1} (Fig. 27, curve 5) in the range 800−1100°C is shown, and then is not substantially reduced, demonstrating the formation of polycrystalline SiC phase at this temperature. In general, for the SiC$_{0.4}$, SiC$_{0.12}$ and SiC$_{0.03}$ layers with low carbon concentration a sharp narrowing of the peak occurs at

temperatures of about 100°C lower than for the layers SiC$_{1.4}$, SiC$_{0.95}$ and SiC$_{0.7}$ due to a lower concentration of strong clusters.

Thus, we have shown a negative effect of stable carbon and carbon-silicon clusters on the crystallization of SiC in the layers. Heat treatment up to 1200°C does not lead to complete disintegration of the clusters and the release of C and Si atoms to form SiC. In this regard, identification of alternative ways of processing the films to break down clusters and form a more qualitative structure of the SiC films is important. As shown in section 3.3, the characteristics of glow discharge hydrogen plasma and treatment (27.12 MHz, 12.5 W, 6.5 Pa, 100°C, 5 min) were sufficient to decay the tetrahedral Si−Si and Si−C-bonds and can be used for the destruction of stable carbon and carbon−silicon clusters. For IR analysis, the sample with the SiC$_{0.95}$ film was cut into two parts and one of these samples was treated by hydrogen plasma. Fig. 28 shows the IR transmittance spectra of these SiC$_{0.95}$ layers, untreated by plasma (a) and treated by hydrogen plasma (b) after annealing at 900°C for 30 minutes.

Peak maxima occur at 790 cm^{-1}, indicating the prevalence of tetrahedral oriented Si−C-bonds characteristic of crystalline SiC. Measurements of the half-widths of the spectra in Fig. 28a, b give the magnitudes 148 and 78 cm^{-1} for pre-untreated and treated by hydrogen plasma SiC$_{0.95}$ layer, respectively. If the value of 148 cm^{-1} is characteristic for the temperature range 900−1000°C (Fig. 27, curve 2), but the value of 78 cm^{-1}, in principle, was unattainable for the SiC$_{0.95}$ layer without pre-treatment by plasma throughout the temperature range 200−1400°C. Thus, we can conclude that annealing at 900°C of SiC$_{0.95}$ layers, treated by hydrogen plasma with power of 12.5 watts only, has led to the formation of β-SiC crystalline layer, which superior in structure quality the untreated by plasma layer subjected to isochronous annealing in the range 200−1400°C. Obviously, the observed effects of plasma-induced crystallization is a consequence of the decay of clusters in the pre-treatment by glow discharge hydrogen plasma.
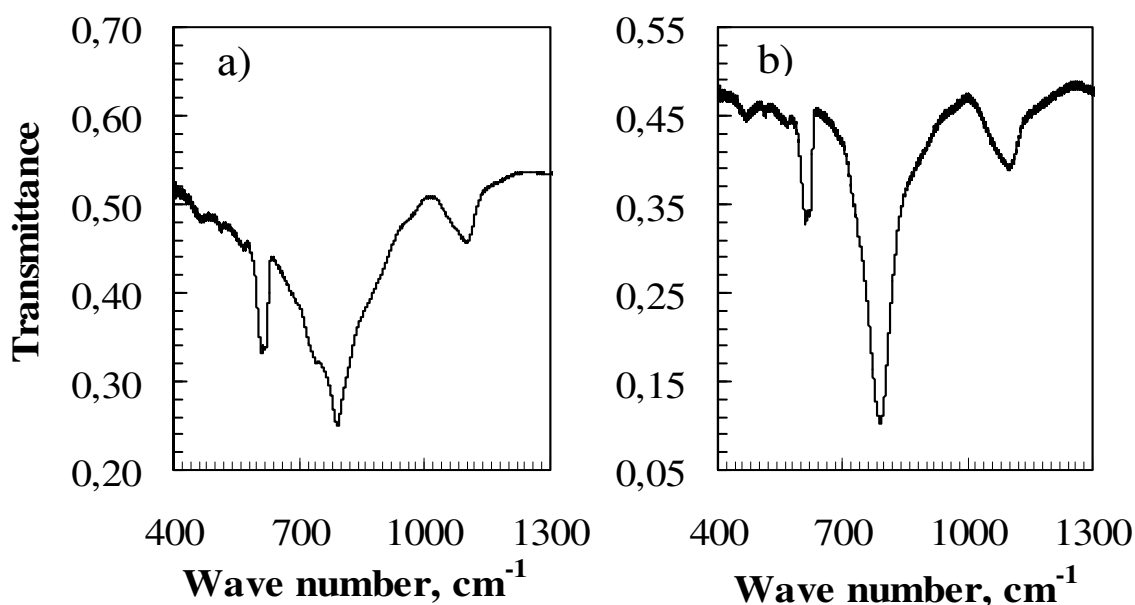

Fig. 28. IR transmission spectra for SiC$_{0.95}$ layer after annealing at the temperature 900°C for 30 min (a) and after processing by glow discharge hydrogen plasma for 5 min and annealing at the temperature 900°C for 30 min (b).

3.5 Investigations by atomic force microscopy

AFM studies of the surface microstructure of the surface of the $SiC_{0.95}$ layer of area 500×500 nm^2, and 1×1 um^2 show (Fig. 29a), that after implantation, the surface of the layer looks flat with fluctuations in the height ranged within 6 nm. The areas above the average line of the surface have bright light colors and the areas below the same have dark colors, from which begins the account of height. Annealing at 800°C (Fig. 29b) leads to the deformation of the surface and to an appearance of furrows indicating an intensive translations of atoms. After annealing at 1400°C the surface consists of grains with sizes of 30−50 nm. The variations in height ranged within 66 nm. Comparison of grain sizes with X-ray data on the average crystallite sizes of SiC (3−10 nm) shows that the grains are composed of crystallites of SiC.
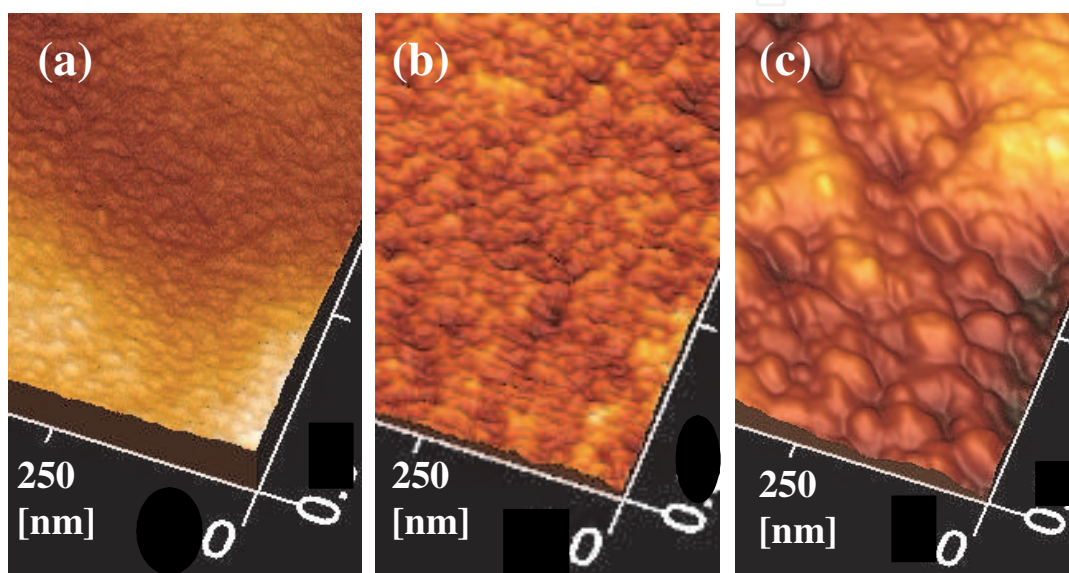

Fig. 29. AFM images from the surface of thin (~130 nm) $SiC_{0.95}$ film (a) after multiple implantation and annealing at (b) 800°C and (c) 1400°C.

In general, we can see that after implantation the surfaces of $SiC_{1.4}$, $SiC_{0.95}$, $SiC_{0.7}$, $SiC_{0.4}$ and $SiC_{0.12}$ layers looks smooth with the fluctuations of the height in range of 2−6 nm (Fig. 30). At temperatures of 800–1400°C the surface of these layers are deformed with the formation of grains with sizes of ~30–100 nm. For example, after implantation the smooth surface of $SiC_{1.4}$ layer looks broken with fluctuations of the height in range of 2 nm. Annealing at 1400°C leads to a clear fragmentation of grains on the surface. It is seen that the grains with sizes of ~100 nm are composed of subgrains, which probably represent the SiC crystallites with an average size of 10 nm. The surface of $SiC_{0.7}$ layer, after annealing at 1250°C for 30 minutes, consists of granules of a size of 50−100 nm and flat areas.

Amorphous after implantation, the surface structure of the $SiC_{0.4}$ layer is also transformed after annealing at 1200°C for 30 minutes and forms a granular structure consisting of spherical grains of Si and SiC with sizes of ~ 50−100 nm, which suggests an intensive movements of atoms in this layer at high temperature due to the lower content of stable clusters in the film. The surface of the $SiC_{0.12}$ layer after annealing at 1400°C consists of grains with sizes of 50 nm. The smooth surface of $SiC_{0.03}$ layer is recrystallized at 1250°C and contains evenly distributed inclusions of SiC in the form of point protrusions with a diameter of 20 nm (Fig. 30).
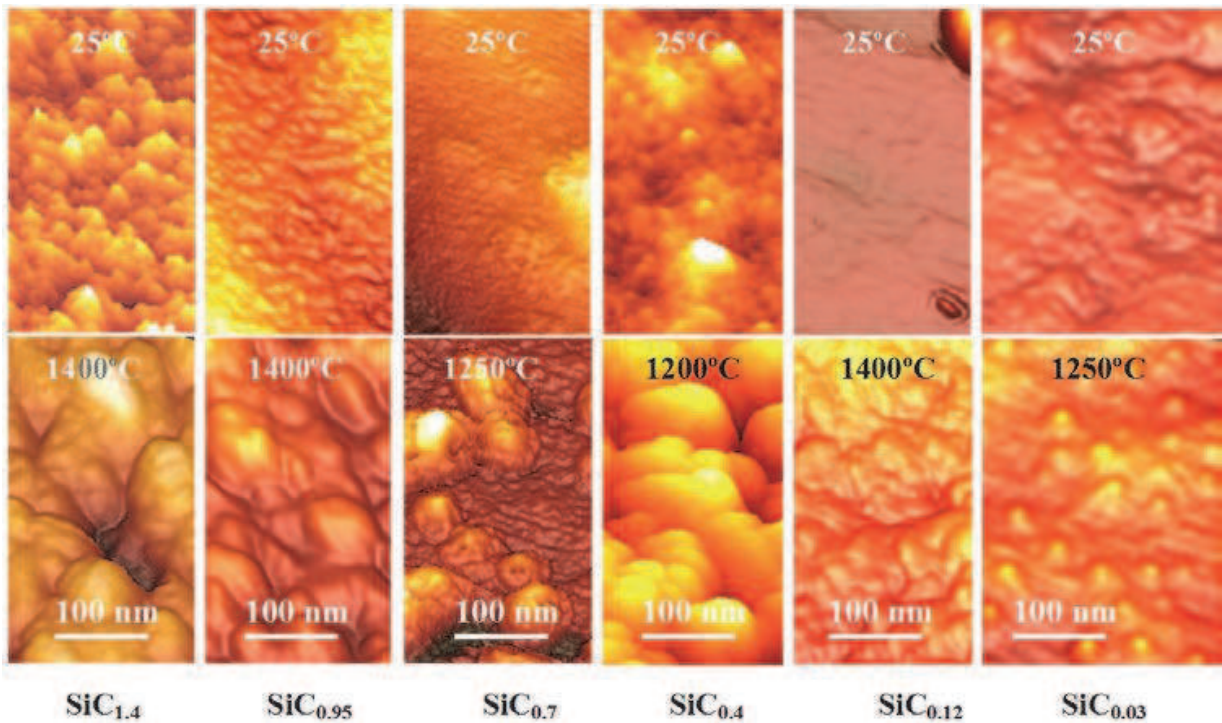
Fig. 30. Atomic force microscopy of the surface of SiC$_x$ layers with various carbon concentration before and after high temperature annealing

In Fig. 31 the AFM data on changes in surface topography of the annealed at 1400°C SiC$_{1.4}$ layer before (Fig. 31a) and after (Fig. 31b and c) processing by glow discharge hydrogen plasma (27.12 MHz, 12.5 W, 6.5 Pa, 100°C, 5 min) in two various areas with sizes of 1 × 1 um², are presented. The more increased fragments are also shown. Processing by hydrogen plasma does not lead to complete destruction of the granular structure (Fig. 31b), although in some areas granular structure significantly damaged (Fig. 31c), which correlates with the X-ray data (Fig. 7).
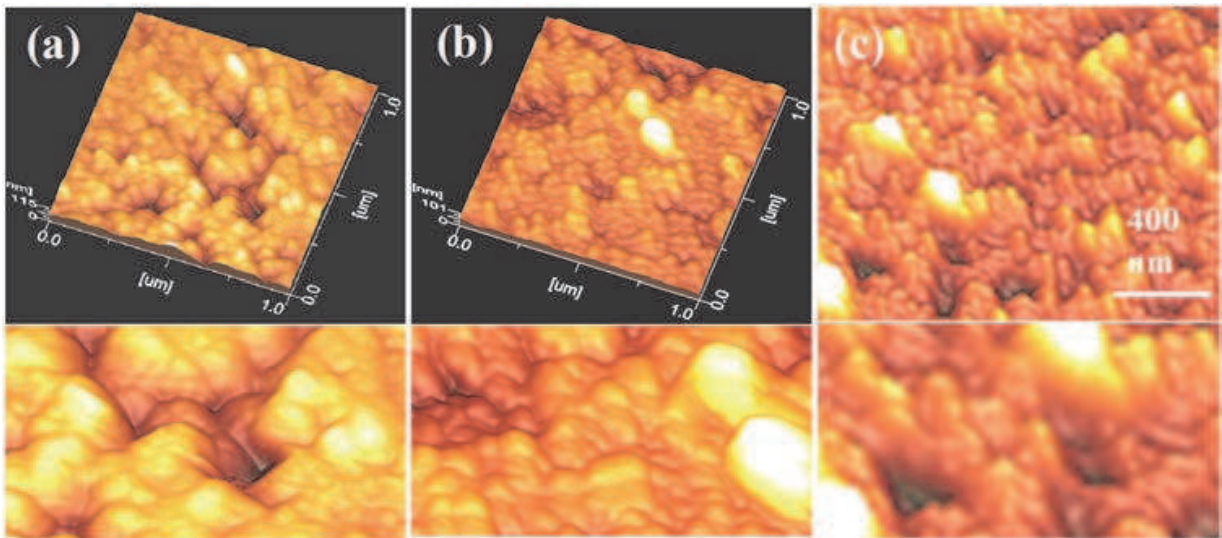

Fig. 31. Atomic force microscopy of SiC$_{1.4}$ layers after annealing at the temperature of 1400°C (a) and subsequent processing by glow discharge hydrogen plasma for 5 min (b, c).

Fig. 32a, b shows the surface areas of the untreated by hydrogen plasma $SiC_{0.95}$ film after annealing at 900°C, which have a granular structure and consist of grains with sizes within ~50−250 nm. On the enlarged fragments one can also see the flat areas which can be associated with the amorphous component. Surface after treatment by glow discharge hydrogen plasma for 5 min and annealing at 900°C has a more developed granular structure (Fig. 32c, d) and consist of grains with sizes within ~150−400 nm. These results correlate with the IR spectroscopy data (Fig. 28).
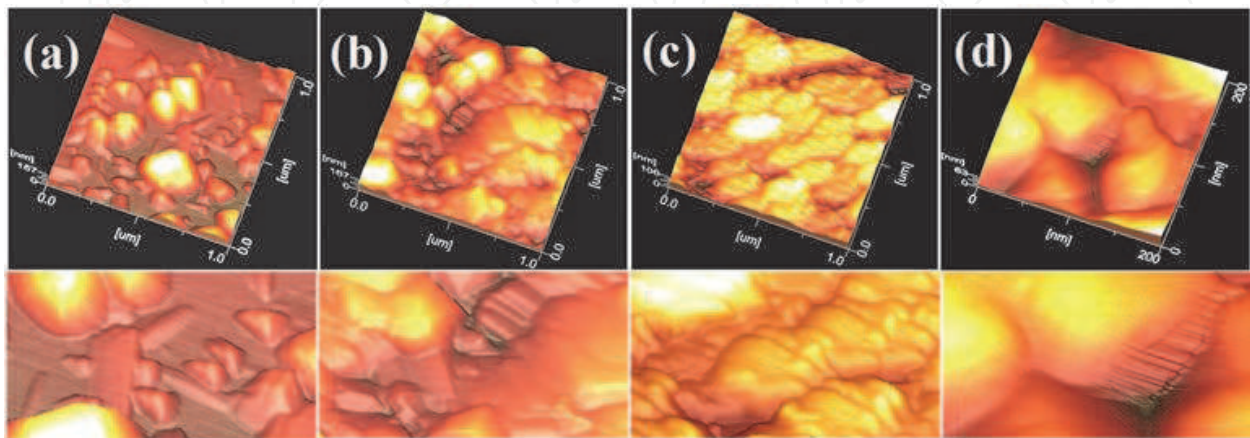

Fig. 32. Atomic force microscopy of $SiC_{0.95}$ layer: (a, b) after synthesis and annealing at the temperature of 900°C for 30 min; (c, d) after synthesis, processing by glow discharge hydrogen plasma for 5 min and annealing at 900°C for 30 min.

4. Conclusion

1. For SiC_x layers, formed by multiple ion implantation in Si of $^+C^{12}$ ions with energies 40, 20, 10, 5 and 3 keV, the regularities of influence of the decay of clusters and optically active bonds on the formation of tetrahedral oriented Si−C-bonds, characteristic of crystalline silicon carbide, were revealed. Formation of these bonds in the $SiC_{1.4}$, $SiC_{0.95}$ and $SiC_{0.7}$ layers with a high carbon concentration occurs mainly as a result of the decay of optically inactive Si–C-clusters in the temperature range 900−1300°C; in $SiC_{0.12}$ and $SiC_{0.4}$ layers – as a result of the decay of clusters in the range of 1200–1300°C and of optically active long single Si–C-bonds in the range of 700–1200°C; in $SiC_{0.03}$ layers – by reducing the number of dangling bonds of carbon atoms in the range 900–1000°C.

2. The values of carbon concentration in silicon and the temperature ranges which are optimal for the formation of SiC, are revealed. After annealing at 1200°C of homogeneous SiC_x layers, largest sizes of spherical, needle- and plate-type SiC grains up to 400 nm and the largest number of tetrahedral oriented Si−C-bonds are observed for the $SiC_{0.7}$ layer, which is due to a low carbon content in the $SiC_{0.03}$, $SiC_{0.12}$ and $SiC_{0.4}$ layers, and a high concentration of strong clusters in the $SiC_{0.95}$ and $SiC_{1.4}$ layers. In the range of 800−900°C the most number of tetrahedral Si−C-bonds is characteristic for $SiC_{0.4}$ layers.

3. A structural model of $SiC_{0.12}$ layer, which shows the changes in phase composition, phase volume and average crystallite size of SiC and Si in the temperature range 20–1250°C, is proposed. After annealing at 1200°C, about 50% of its volume, free from

Si–C-clusters, is consisted of Si crystallites with average size ~25 nm, 25% of the volume − β-SiC crystallite with size of ~5 nm and 25% − the c-Si recrystallized near the transition "film − substrate".

4. The regularities of changes in the surface structure of the SiC$_x$ layers (x = 0.03–1.4) with the increase of temperature are revealed. At temperatures of 800–1400°C the surface layers are deformed with the formation of grains with sizes of ~30–100 nm, consisting of crystallites, and the recrystallized at 1250°C smooth surface of SiC$_{0.03}$ layer contains evenly distributed Si:C inclusions in the form of point protrusions with a diameter of ~20 nm.

5. Size effects were revealed, which manifested in the influence of the crystallite sizes of silicon carbide on its optical properties. The differences of the SiC$_{0.03}$, SiC$_{0.12}$ and SiC$_{0.4}$ layers with low carbon concentration from the SiC$_{1.4}$, SiC$_{0.95}$ and SiC$_{0.7}$ layers with high carbon concentration are manifested in the absence of LO-phonon peak of SiC in the IR transmission spectra and in a shift at 1000°C of minimum SiC-peak for TO phonons in the region of wave numbers higher than 800 cm^{-1} characteristic for the tetrahedral bonds of crystalline SiC, which is caused by small sizes of SiC crystallites ($\leq$ 3 nm) and by an increase of contribution in the IR absorption of their surfaces, and the surfaces of Si crystallites containing strong short Si−C-bonds as well.

6. The estimations of the proportion of carbon atoms that form clusters in the SiC$_x$ layers are evaluated. At 1300°C in the SiC$_{1.4}$ layer only ~9% of C atoms form the optically active Si–C-bonds, in SiC$_{0.95}$ − 12%, in SiC$_{0.7}$ and SiC$_{0.4}$ − 16%, in SiC$_{0.12}$ − 45%, while the remaining carbon atoms are included in composition of stable clusters. The total number N of formed Si–C-bonds in SiC$_x$ layers was growing with a fractional power of carbon concentration x: $N = a \cdot (n_1)^y$, where $y \approx 0.37 \pm 0.09$, $n_1 = x/0.03$, a = const.

7. It was shown that processing by hydrogen glow discharge plasma (27.12 MHz, 12.5 W, 6.5 Pa, 100°C, 5 min) of polycrystalline SiC$_{1.4}$ layer leads to partial disintegration of β-SiC crystallites in layer and complete decay of Si crystallites in the transition layer "film−substrate" ("SiC−Si"). Processing by plasma and annealing at 900°C of SiC$_{0.95}$ layer has led to the formation of β-SiC crystalline layer, which superior in structure quality the untreated by plasma layer subjected to isochronous annealing in the range 200−1400°C. Phenomenon of plasma-induced crystallization is a consequence of the decay of clusters during pre-treatment by glow discharge hydrogen plasma.

5. Acknowledgement

6. References

Akimchenko, I.P., Kisseleva, K.V., Krasnopevtsev, V.V., Milyutin, Yu.V., Touryanski, A.G., Vavilov, V.S. (1977). The structure of silicon carbide synthesized in diamond and silicon by ion implantation. Radiation Effects, Vol. 33., pp.75–80.

Akimchenko, I.P., Kazdaev, H.P., Krasopevtsev, V.V. (1977). IK-pogloshenie β-SiC, sintezirovannogo pri ionnoi implantacii C v Si. Fizika i Tekhnika Poluprovodnikov, T.11, vyp. 10., pp.1964-1966 (in Rusiian).

Akimchenko, I.P., Kazdaev, H.R., Kamenskikh, I.A., Krasnopevtsev, V.V. (1979). Opticheskie i fotoelektricheskie svoistva struktury SiC−Si, poluchennoi pri implantacii ionov ugleroda v kremnii. Fizika i Tekhnika Poluprovodnikov, T.13, vyp.2., pp. 375-378 (in Rusiian).

Akimchenko, I.P., Kisseleva, K.V., Krasnopevtsev, V.V., Touryanski, A.G., Vavilov, V.S. (1980). Structure and optical properties of silicon implanted by high doses of 70 and 310 keV carbon ions. Radiation Effects, Vol. 48., pp.7–12.

Aleksandrov, P.A., Baranova, E.K., Demakov, K.D., Komarov, F.F., Novikov, A.P., Shiryaev, S.Y. (1986). Sintez monokristallicheskogo karbida kremniya s pomoshyu odnoshagovoi tehniki vysokointensivnogo ionnogo legirovaniya. Fizika i Tekhnika Poluprovodnikov, T.20, v.1, pp. 149-152 (in Rusiian).

Baranova, E.K., Demakov, K.D., Starinin, K.B., Strelcov, L.N., Haibullin, I.B. (1971). Issledovanie monokristallicheskih plenok SiC, poluchennykh pri bombardirovke ionami C+ monokristallov Si. Doklady AN SSSR, vol. 200, pp. 869-870 (in Rusiian).

Bayazitov, R.M., Haibullin, I.B., Batalov, R.I., Nurutdinov, R.M. (2003a). Formation of cubic silicon carbide layers on silicon under the action of continuous and pulsed carbon ion beams. Technical Physics, Vol. 48, iss. 6, pp. 742-744.

Bayazitov, R.M., Haibullin, I.B., Batalov, R.I., Nurutdinov, R.M., Antonova, L.Kh., Aksenov, V.P., Mikhailova, G.N. (2003b) Structure and photoluminescent properties of SiC layers on Si, synthesized by pulsed ion-beam treatment. Nucl. Instrum. and Meth. in Phys. Res. B., V. 206, pp. 984-988.

Belov, A.I., A.N. Mihailov, D.E. Nikolichev, A.V. Boryakov, A.P. Sidorin, A.P. Grachev, A.V. Ershov, D.I. Tetelbaum (2010). Formation and "white" photoluminescence of nanoclusters in SiO_x films implanted with carbon ions. Semiconductors. Vol. 44, iss. 11, pp. 1450-1456.

Burenkov, A.F., Komarov, M.A., Temkin, M.M. (1985). In: Prostranstvennye raspredeleniya energii, vydelennoi v kaskade atomnyx stolknovenii v tverdyx telax, Energoizdat., 245 c. (in Rusiian).

Borders, J.A., Picraux, S.T. and Beezhold, W. (1971). Formation of SiC in silicon by ion implantation. Appl.Phys.Lett., Vol. 18, iss. 11., pp.509–511.

Calcagno, L., Compagnini, G., Foti, G., Grimaldi, M.G., Musumeci, P. (1996). Carbon clustering in $Si_{1-x}C_x$ formed by ion implantation. Nucl.Instrum. and Meth. in Phys.Res., B 120, pp.121 – 124.

Chen, D., Cheung, W.Y., Wong, S.P (1999). Ion beam induced crystallization effect and growth kinetics of buried SiC layers formed by carbon implantation into silicon. Nucl. Instrum. and Meth. in Phys.Res., B148, pp. 589–593.

Chen D., Wong, S.P., Yang Sh., Mo D. (2003). Composition, structure and optical properties of SiC buried layer formed by high dose carbon implantation into Si using metal vapor vacuum arc ion source. Thin Solid Films, Vol. 426, pp.1–7.

Durupt, P., Canut, B., Gauthier, J.P., Roger, J.A. and Pivot, J (1980). RBS, infrared and diffraction compared analysis of SiC synthesis in C implanted silicon. Mater. Res. Bull, 15, pp. 1557–1565.

Edelman, F.L., Kuznetsov, O.N., Lezheiko, L.V. and Lubopytova, E.V. (1976). Formation of SiC and Si_3N_4 in silicon by ion implantation. Radiation Effects, 29, pp. 13–15.

Fan, J.Y., Wu, X.L., Chu, P.K. (2006). Low-dimensional SiC nanostructures: Fabrication, luminescence, and electrical properties. Prog.Mater.Sci., Vol. 51., pp. 983–1031.

Fissel, A., Kaizer, U., Schroter, B., Richter, W., Bechstedt, A. (2001). MBE growth and properties of SiC multi-quantum well structures. Applied Surface Science, 184, iss. 1, pp. 37–42.

Fissel, A., Kaizer, U., Pfennighaus, K., Schroter, B., Richter, W. (1996). Growth of 6H–SiC on 6H–SiC(0001) by migration enhanced epitaxy controlled to an atomic level using surface superstructures. Applied Physics Letters, 68, pp. 1204–1206.

Fissel, A., Schroter, B., Kaiser, U., Richter, W. (2000). Advances in the molecular-beam epitaxial growth of artificially layered heteropolytypic structures of SiC. Appl. Phys. Lett., Vol. 77., pp. 2418-2420.

Frangis, N., Stoemenos, J., Van Landuyt, J., Nejim, F., Hemment, P.L.F. (1997). The formation of 3C-SiC in crystalline Si by carbon implantation at 950ºC and annealing – a structural study. Journal of Crystal Growth, 181, pp.218–228.

George, V.C., Das, A., Roy, M., Dua, A.K., Raj, P., Zahn, D.R.T. (2002). Bias enhanced deposition of highly oriented β-SiC thin films using low pressure hot filament chemical vapour deposition technique. Thin Solid Films, Vol. 419, pp. 114–117.

Gerasimenko, N.N., Kuznetsov, O.N., Lezheyko, L.V., Lyubopytova, E.V., Smirnov, L.S., Edelman, F.L. (1974). Nekotorye svoistva plenok SiC, poluchennykh ionnym vnedreniem v strukture Al-SiC-Si. Mikroelektronika, T.3., Vyp.5, pp. 467-468 (in Rusiian).

Gibbons, J.F., Johnson, W.S. and Mylroic, S.W. (1975). Projected Range Statistics. Part 1. 93 p. 2nd ed. Dowden, Stroudsburg. PA.

Gonzalez-Varona, O., Perez-Rodriguez, A., Garrido, B., Bonafos, C., Lopez, M., Morante, J.R., Montserrat, J., Rodrguez, R. (2000). Ion beam synthesis of semiconductor nanoparticles for Si based optoelectronic devices. Nucl. Instrum. Methods Phys. Res., B, V. 161–163, pp. 904–908.

Kantor, Z., Fogarassy, E., Grob, A., Grob, J.J., Muller, D., Prevot, B., Stuck, R. (1997). Evolution of implanted carbon in silicon upon pulsed excimer laser annealing: epitaxial Si$_{1-y}$C$_y$ alloy formation and SiC precipitation. Appl. Surf. Sci., 109/110, pp. 305-311.

Kerdiles, S., Rizk, R., Gourbilleau, F., Perez-Rodriguez, A., Garrido, B., Gonzalez-Varona, O., Morante, J.R. (2000). Low temperature direct growth of nanocrystalline silicon carbide films. Mater.Sci.Eng., B, Vol.69, pp. 530–535.

Khohlov, A.F., Pavlov, D.A., Mashin, A.I., Mordvinova, Y.A. (1987). Izovalentnoe legirovanie amorphnogo kremniya uglerodom. Fizika I tehnika poluprovodnikov,, T.21, vyp.3, pp. 531-535 (in Rusiian).

Kimura, T., Kagiyama, Sh. and Yugo, Sh. (1984). Auger electron spectroscopy analysis of SiC layers form by carbon ion implantation into silicon. Thin Solid Films, Vol. 122, pp.165–172.

Kimura, T., Kagiyama, Sh. and Yugo, Sh. (1982). Characteristics of the synthesis of β-SiC by the implantation of carbon ions into silicon. Thin Solid Films, Vol. 94, pp.191–198.

Kimura, T., Kagiyama, Sh. and Yugo, Sh. (1981). Structure and annealing properties of silicon carbide thin layers formed by ion implantation of carbon ions in silicon. Thin Solid Films, 81, pp.319–327.

Lebedev, A.A., Mosina, G.N., Nikitina, I.P., Savkina, N.S., Sorokin, L.M., Tregubova, A.C. (2001). Investigation of the structure of (p)3C-SiC-(n)6H-SiC. Tech. Phys. Lett., Vol. 27, P. 1052-1054.

Lebedev, A.A., Strel'chuk, A.M., Savkina, N.S., Bogdanova, E.V., Tregubova, A.S., Kuznetsov, A.N., Sorokin, L.M. (2002a). Investigation of the p⁻-3C-SiC/n⁺-6H-SiC heterostructures with modulated doping. Tech. Phys. Lett., Vol. 28, iss. 12, p. 1011-1014.

Lebedev, A.A., Strel'chuk, A.M., Davydov, D.V., Savkina, N.S., Kuznetsov, A.N., Sorokin, L.M. (2002b). Electrical characteristics of (p)3C-SiC–(n)6H-SiC heterojunctions. Tech. Phys. Lett., Vol. 28, iss.9, pp. 792-794.

Lebedev, A.A., Nelson, D.K., Razbirin, B.S., Saidashev, I. I., Kuznetsov, A.N., Cherenkov, A. E. (2005) Study of the properties of two-dimensional electron gas in p⁻-3C-SiC/n+-6H-SiC heterostructures at low temperatures. Semiconductors, Vol. 39, iss.10, P. 1194-1996.

Liangdeng, Y., Intarasiri, S., Kamwanna, T., Singkarat, S. (2008). Ion beam synthesis and modification of silicon carbide. In book "Ion beam applications in surface and bulk modification of insulators". - IAEA, Austria, Vienna, IAEA-TECDOC-1607. - P.63-92.

Liao, F., Girshick, S.L., Mook, W.M., Gerberich, W.W., Zachariah, M.R. (2005). Superhard nanocrystalline silicon carbide films. Appl. Phys. Lett., Vol. 86, pp. 171913–171915.

Lindner, J.K.N. (2003). High-dose carbon implantations into silicon: fundamental studies for new technological tricks. Appl.Phys. A., Vol. 77, pp. 27-38.

Lindner, J.K.N., Volz, K., Preckwinkel, U., Gotz, B., Frohnwieser, A. Stritzker, B., Rauschenbach, B. (1996). Formation of buried epitaxial silicon carbide layers in silicon by ion beam synthesis. Materials Chemistry and Physics,46 (2-3), pp.147-155.

Mandal, S., Seal, A., Dalui, S.K., Dey, A.K., Ghatak, S. and Mukhopadhyay, A.K. (2001). Mechanical characteristics of microwave sintered silicon carbide. Bull. Mater. Sci., V. 24, № 2, pp. 121–124.

Martin, P., Daudin, B., Dupuy, M., Ermolieff, A., Olivier, M., Papon, A.M. and Rolland, G. (1990). High temperature ion beam synthesis of cubic SiC. J. Appl. Phys., 67 (6), pp.2908–2912.

Nishino, S., Jacob, C., Okui, Y. (2002). Lateral over-growth of 3C-SiC on patterned Si(111) substrates. Journal of Crystal Growth, 237–239, pp. 1250–1253.

Pajagopalan, T., Wang, X., Lanthouh, B., Ramkumar, C. (2003). Low temperature deposition of nanocrystalline silicon carbide films by plasma enhanced chemical vapor deposition and their structural and optical characterization. J. Appl. Phys., Vol.94, iss.3., pp. 5252–5260.

Perez-Rodrıguez, A., Gonzalez-Varona, O., Garrido, B., Pellegrino, P., Morante, J.R., Bonafos, C., Carrada, M., Claverie, A. (2003). White luminescence from Si⁺ and C⁺ ion-implanted SiO₂ films. J. Appl. Phys., V. 94., 1., pp. 254–262.

Preckwinkel U., Lindner, J.K.N., Stritzker B., Rauschenbach B. (1996). Structure and strain measurements on SiC formed by carbon ion implantation. Nucl. Instrum. and Meth. in Phys.Res., B 120, pp. 125–128.

Reeson, M., Stoemenos, J., Hemment, P.L.F. (1990). Mechanism of buried β-SiC formation by implanted carbon in silicon. Thin Solid Films, Vol. 191, pp. 147–164.

Rothemund, W., Fritzsche, C.R. (1974). Optical absorption and electrical conductivity of SiC films produced by ion implantation J.Electrochem. Soc.: Solid-state science and technology, Vol. 121, №4., pp. 586–588.

Savkina, N.S., Lebedev, A.A., Davydov, D.V., Strelchuk, A.M., Tregubova, A.S., Raynaud, C., Chante, J.P., Locatelli, M.L., Planson, D., Nilan, J., Godignon, P., Campos, F.J., Nestres, N., Pascual, J., Brezeanu, G., Batila, M. (2000). Low-doped 6H-SIC n-type epilayers grown by sublimation epitaxy. Materials Science and Engineering, B77, pp. 50–54.

Semenov, A.V., Puzikov, V.M., Dobrotvorskaya, M.V., Fedorov, A.G., Lopin, A.V. (2008). Nanocrystalline SiC films prepared by direct deposition of carbon and silicon ions. Thin Solid Films, Vol. 516, iss.10., pp. 2899–2903.

Semenov, A.V., Puzikov, V.M., Golubova, E.P., Baumer, V.N., Dobrotvorskaya, M.V. (2009). Low-temperature production of silicon carbide films of different polytypes. Semiconductors, Vol. 43, iss. 5, pp. 685-689.

Semenov, A.V. Lopin, A.V, Puzikov, V.M., Baumer, V.N., Dmitruk, I.N. (2010). Fabrication of heterostructures based on layered nanocrystalline silicon carbide polytypes. Semiconductors, Vol. 44, iss. 6, pp. 816-823.

Serre, C., Romano-Rodríguez, A., Pérez-Rodríguez, A., Morante, J. R., Fonseca, L., Acero, M.C., Kögler, R. and Skorupa, W. (1999). β-SiC on SiO$_2$ formed by ion implantation and bonding for micromechanics applications. Sensors and Actuators A: Physical, 74, 1–3, pp. 169–173.

Shimizu-Iwayama, T., Nakao, S., Saitoh, K. (1994). Visible photoluminescence in Si+-implanted thermal oxide films on crystalline Si. Appl. Phys. Lett., Vol.65(14), pp.1814–1816.

Silverstein, R., Bassler, G., Morril, T. (1988). Spektrometricheskaya identifikaciya organicheskih soedinenii. M: Mir, 590 s. (in Rusiian).

Simon, L., Faure, J., Mesli, A., Heiser, T., Grob, J.J., Balladore, J.L. (1996). XTEM and IR absorption analysis of silicon carbide prepared by high temperature carbon implantation in silicon. Nucl.Instrum. and Meth. in Phys.Res., B 112, pp. 330-333.

Singh, S.K., Mohanty, B.C. and Basu, S. (2002). Synthesis of SiC from rice husk in a plasma reactor. Bull.Mater.Sci., V. 25, № 6, pp. 561–563.

Spillman, H., Wilmott, P.R. (2000). Growth of SiN$_x$ and SiC$_x$ thin films by pulsed reactive crossed-beam laser ablation. Applied Physics. A. - Materials Science & Processing, Vol. 70., Iss. 3., pp. 323–327.

Srikanth, K., Chu, M., Ashok, S., Nguyen, N., Vedam, K. (1988). High-dose carbon ion implantation studies in silicon. Thin Solid Films, 163, pp.323–329.

Sun, Y., Miyasato, T.J.(1988). Characterization of cubic SiC films grown on thermally oxidized Si substrate. J. Appl. Phys., Vol. 84., pp. 2602–2611.

Tetelbaum, D.I., Mikhaylov, A.N., Belov, A.I., Vasiliev, V.K., Kovalev, A.I., Wainshtein, D.L., Golan, Y., Osherov, A. (2009). Luminescence and structure of nanosized inclusions formed in SiO$_2$ layers under double implantation of silicon and carbon ions. Journal of Surface Investigation. X-ray, Synchrotron and Neutron Techniques, Vol. 3, № 5, pp. 702–708.

Theodossiu, E., Baumann, H. and Bethge, K. (1999). Formation of SiC surface layer by ion implantation. J. Appl. Phys., 86., pp. 4703–4705.

Wong, S.P., Chen, D., Ho, L.C., Yan, H., Kwok, R.W.M. (1998). Infrared absorption spectroscopy study of phase formation in SiC layers synthesized by carbon implantation into silicon with a metal vapor vacuum arc ion source. Nucl. Instrum. and Meth. in Phys.Res., B140, pp.70–74.

Yan, H., Wang, B., Song, X.M., Tan, L.W., Zhang, S.J., Chen, G.H., Wong, S.P., Kwok, R.W.M., Leo, W.M.L. (2000). Study on SiC layers synthesized with carbon ion beam at low substrate temperature. Diamond and related materials, Vol. 9, pp. 1795–1798.

Zhao, J., Mao, D.S., Lin, Z.X., Jiang, B.Y., Yu, Y.H., Liu, X.H., Wang, H.Z. and Yang, G.Q. (1998). Intense short wavelength photoluminescence from thermal SiO_2 films co-implanted with Si and C ions. Appl. Phys. Lett., V. 73, №13, pp. 1838–1840.
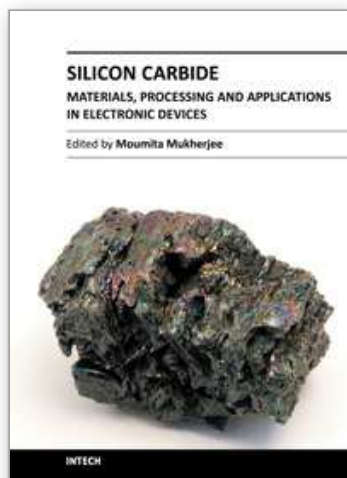
Silicon Carbide - Materials, Processing and Applications in Electronic Devices

Edited by Dr. Moumita Mukherjee

ISBN 978-953-307-968-4

Hard cover, 546 pages

Publisher InTech

Published online 10, October, 2011

Published in print edition October, 2011

Silicon Carbide (SiC) and its polytypes, used primarily for grinding and high temperature ceramics, have been a part of human civilization for a long time. The inherent ability of SiC devices to operate with higher efficiency and lower environmental footprint than silicon-based devices at high temperatures and under high voltages pushes SiC on the verge of becoming the material of choice for high power electronics and optoelectronics. What is more important, SiC is emerging to become a template for graphene fabrication, and a material for the next generation of sub-32nm semiconductor devices. It is thus increasingly clear that SiC electronic systems will dominate the new energy and transport technologies of the 21st century. In 21 chapters of the book, special emphasis has been placed on the "materials" aspects and developments thereof. To that end, about 70% of the book addresses the theory, crystal growth, defects, surface and interface properties, characterization, and processing issues pertaining to SiC. The remaining 30% of the book covers the electronic device aspects of this material. Overall, this book will be valuable as a reference for SiC researchers for a few years to come. This book prestigiously covers our current understanding of SiC as a semiconductor material in electronics. The primary target for the book includes students, researchers, material and chemical engineers, semiconductor manufacturers and professionals who are interested in silicon carbide and its continuing progression.

How to reference

In order to correctly reference this scholarly work, feel free to copy and paste the following:

Kair Kh. Nussupov and Nurzhan B. Beisenkhanov (2011). The Formation of Silicon Carbide in the SiCx Layers (x = 0.03–1.4) Formed by Multiple Implantation of C Ions in Si, Silicon Carbide - Materials, Processing and Applications in Electronic Devices, Dr. Moumita Mukherjee (Ed.), ISBN: 978-953-307-968-4, InTech, Available from: http://www.intechopen.com/books/silicon-carbide-materials-processing-and-applications-in-electronic-devices/the-formation-of-silicon-carbide-in-the-sicx-layers-x-0-03-1-4-formed-by-multiple-implantation-of-c-

Fax: +385 (51) 686 166   Fax: +86-21-62489821
www.intechopen.com